G-baToN: a versatile cell-cell interaction reporter system

Rui Tang[1*], Christopher W. Murray[2], Ian Linde[4], Nicholas J. Kramer[1,3], Min K. Tsai[1], Leo Chen[1], Hongchen Cai[1], Aaron D. Gitler[1,3], Edgar Engleman[2,4,5], and Monte M. Winslow[1,2,5*]

[1] Department of Genetics, Stanford University School of Medicine, Stanford, CA, USA

[2] Cancer Biology Program, Stanford University School of Medicine, Stanford, CA, USA

[3] Neuroscience Program, Stanford University School of Medicine, Stanford, CA, USA

[4] Immunology Program, Stanford University School of Medicine, Stanford, CA, USA

[5] Department of Pathology, Stanford University School of Medicine, Stanford, CA, USA

* Corresponding authors: Rui Tang: tangrui@stanford.edu and Monte M. Winslow: mwinslow@stanford.edu

ABSTRACT

Cell-cell interactions influence all aspects of development, homeostasis, and disease. Here, we describe GFP-based Touching Nexus (G-baToN) which relies upon fluorescent protein transfer driven by nanobody-mediated recognition to enable sensitive and specific labeling of cells after cell-cell interactions. A suite of orthogonal baToN tools enables reciprocal cell-cell labeling, interaction-dependent cargo transfer, and the identification of higher order cell-cell interactions across a wide range of cell types.

17

18 **MAIN TEXT**

19 Cell-cell interactions contribute to almost all physiological and pathological states.
20 Despite the explosion of interest in uncovering and understanding cell heterogeneity in tissues
21 and across disease states, the extent to which cell-cell interactions influence cell state, drive
22 heterogeneity, and enable proper tissue function remains poorly understood[1, 2]. Detailed analysis
23 of the impact of defined cell-cell interactions has illuminated critical aspects of biology, however,
24 these analyses have been limited to a small collection of signaling interfaces engaged by direct
25 cell-cell contact that are tractable to study. Molecular methods to profile cell state, including *in*
26 *situ* approaches within intact tissue architecture, largely fail to uncover the causal relationship of
27 cell-cell interactions with the underlying biology[3, 4]. Computational and experimental methods to
28 characterize cell-cell interactions yield additional layers of dimensionality, however, modalities
29 to capture cell-cell interactions are limited[5-7] (Supplementary Fig. 1). Much as diverse systems to
30 detect and quantify protein-protein interactions have revolutionized our biochemical
31 understanding of molecular systems, the development of novel systems to detect and quantify
32 cell-cell interactions should help to map the interaction networks of multicellular systems
33 (Supplementary Fig. 1).

34 Endogenous cell-cell interactions can result in the transfer of surface proteins between
35 cells, thus we sought to couple this phenomenon with fluorescent protein tagging as a means of
36 labeling cells that have undergone direct interaction with a neighboring cell[8-10]. Specifically, we
37 adapted an engineered surface protein/ligand system based on the expression of surface GFP
38 (sGFP) on sender cells and a cell surface anti-GFP (αGFP) nanobody on receiver cells[6, 11, 12]. Co-
39 culturing sGFP sender cells with αGFP receiver cells led to GFP transfer and labeling of the

40 receiver cells (Fig. 1a, b and Supplementary Fig. 1). Receiver cell labeling required direct cell-
41 cell contact, active membrane dynamics, and pairing between sGFP and its cognate αGFP
42 receptor (Fig. 1c, d and Supplementary Fig. 2b, c). Interestingly, sGFP transfer was accompanied
43 by reduced GFP on the sender cells, downregulation of αGFP from the surface of the receiver
44 cells and was partially blocked by chemical inhibitors of endocytosis – all consistent with active
45 and extensive GFP transfer from sender to receiver cells (Supplementary Fig. 2d-f). Thus, this
46 simple system (which we term GFP-based Touching Nexus or G-baToN) enables robust and
47 efficient labeling of predefined receiver cells that have interacted with sender cells.

48 To further characterize the interaction reporter system, we deconstructed the G-baToN
49 design into three functional modules. We found that both the αGFP and sGFP transmembrane
50 domains influence GFP transfer efficiency (Supplementary Fig. 3a-c, g-h). Furthermore, the
51 affinity of the GFP-αGFP pairing impacted GFP transfer (Supplementary Fig. 3d-f). Thus, the
52 analysis of different transmembrane domains on sGFP and αGFP as well as different αGFP
53 nanobodies enabled the identification of combinations that improve unidirectional receiver cell
54 labeling.

55 To characterize the kinetics of G-baToN-mediated receiver cell labeling, we performed
56 co-culture time course experiments with time-lapse imaging and flow cytometry readouts. Time-
57 lapse imaging showed rapid transfer and internalization of GFP by receiver cells (Fig. 1e and
58 Supplementary Movie 1). GFP transfer could be detected within five minutes of co-culture and
59 was half-maximal after six hours (Fig. 1f and Supplementary Fig. 2g). Importantly, GFP
60 fluorescence in receiver cells decayed rapidly after isolation of touched receiver cells from
61 sender cells, thus documenting the transient "real-time" labeling of receiver cells (Supplementary
62 Fig. 2h). To determine the sensitivity of this system, we co-cultured receiver cells with different

63 numbers of sender cells. The fraction of labeled receiver cells was proportional to the number of
64 sender cells and even the addition of very few sender cells (representing less than 1 sender
65 cell/10^5 receiver cells) was sufficient to label rare receiver cells (Fig. 1g, h). Thus, the transfer of
66 GFP to αGFP-expressing cells is a rapid and sensitive method to mark cells that have physically
67 interacted with a predefined sender cell type.

68 Given the high efficiency with which sGFP labels receiver cells upon interaction with
69 cognate sender cells, we tested whether other surface antigen/antibody pairs could lead to protein
70 transfer and labeling. Due to the cross reactivity of αGFP with BFP, co-culture of surface BFP
71 (sBFP) sender cells with αGFP receiver cells generated BFP-labeled receivers[11] (Supplementary
72 Fig. 4a, b). Orthogonal systems consisting of surface-mCherry/αmCherry (LaM4)[11] and surface-
73 GCN4-GFP/αGCN4 (single-chain variable fragment, scFV)[13] also led to efficient and specific
74 receiver cell labeling (Supplementary Fig. 4c-f).

75 We then integrated these orthogonal baToN systems to enable reciprocal labeling and
76 detection higher order multi-cellular interactions. Engineering cells with baToN systems in an
77 anti-parallel fashion should enable reciprocal labeling of both interacting cells. Co-culture of
78 cells expressing sGFP and αmCherry with cells expressing smCherry and αGFP resulted in
79 reciprocal labeling of both interacting cell types (Supplementary Fig. 5a-c). Using orthogonal
80 ligand-receptor pairs, we also created an AND gate dual labeling strategy. Specifically, co-
81 expression of αmCherry and αGFP on receiver cells enabled dual color labeling of receiver cells
82 that had interacted with smCherry-expressing, sGFP-expressing, or both sender cell types (Fig.
83 2a, b, Supplementary Fig. 5d). Analogously, we achieved dual color labeling of receiver cells by
84 leveraging the ability of αGFP to bind both sGFP and sBFP (Supplementary Fig. 5e, f). Thus,

85 derivatives of the G-baToN system allow for additional degrees of resolution of complex cell-
86 cell interactions.

87 Given the high efficiency of protein transfer using the G-baToN system, we also
88 investigated whether cargo proteins could be co-transferred with GFP from sender cells to
89 receiver cells. Initially, we generated sender cells with surface expression of a GFP-tdTomato
90 fusion protein (sGFP-Tom) and uncovered stoichiometric tdTomato and GFP transfer to αGFP
91 receiver cells (Supplementary Fig. 6a, b). We extended this system further by generating sender
92 cells expressing the HaloTag protein fused to sGFP (sHalo-GFP; Fig. 2c)[14]. Covalent attachment
93 of a fluorescent synthetic ligand to sHalo-GFP enabled specific loading onto sender cells
94 (Supplementary Fig. 7a). Co-culture of Alexa Fluor 660 (AF660)-loaded sHalo-GFP sender cells
95 with αGFP receiver cells enabled co-transfer of both GFP and AF660 (Fig. 2d and
96 Supplementary Fig. 7b). Compared to GFP, transfer of the chemical fluorophore using sHalo-
97 GFP-based labeling of receiver cells led to increased foreground to background and higher
98 sensitivity (Fig. 2d and Supplementary Fig. 7c). Importantly, changing from a protein (GFP) to a
99 chemical fluorophore also extended the half-life of labeling, thus enabling partially tunable
100 perdurance of labeling after touching (Supplementary Fig. 7d).

101 Next, we coupled the enhanced properties of chemical fluorophore-based labeling with
102 the generalizability of the GCN4-baToN system to assemble a robust and versatile system to
103 label receiver cells that have interacted with two or more different sender cell types (Fig. 2e, f).
104 Co-culturing αGCN4 receiver with AF488- and AF660-loaded sGCN4-Halo sender cells
105 generated receiver cells with varying degrees of AF488 and AF660 labeling (Supplementary Fig.
106 7e). Importantly, the ratio of AF488 to AF660 transferred to the dually labeled receiver cells
107 strongly correlates with the ratio of the two sGCN4-Halo sender populations within the co-

108 culture, suggesting that this system can quantitively measure higher order cell-cell interactions
109 (Fig. 2f).

110 Beyond fluorescent labels, we tested whether other cargo could be transferred to receiver
111 cells. We generated sGFP-PuroR-expressing sender cells and found that co-culture of sGFP-
112 PuroR sender cells with αGFP receiver cells led to moderate puromycin resistance of touched
113 receiver cells (Supplementary Fig. 6c-e). Furthermore, loading of sGCN4-HaloTag sender cells
114 with biotinylated ssDNA and subsequent staining with streptavidin-conjugated AF647 prior to
115 co-culture with αGCN4 receiver cells revealed successful co-transfer of fluorescently labeled
116 ssDNA (Fig. 2g, h and Supplementary Fig. 7f-g). Thus, baToN systems can achieve contact-
117 dependent transport of different macromolecules between cells.

118 To assess the generalizability of the G-baToN system across cell types, we expressed
119 αGFP on a panel of cell lines and primary cells. Each receiver cell type was able to uptake GFP
120 from sGFP-expressing KPT sender cells upon cell-cell contact (Fig. 3a). Furthermore, diverse
121 sender cancer cell lines and primary cell types expressing sGFP were able to transfer GFP to
122 αGFP-expressing 293 receiver cells (Fig. 3b, Supplementary Fig. 8). Cancer cells undergo
123 interactions with a variety of cell types within primary tumors as well as at metastatic sites. Co-
124 culturing sGFP-expressing lung cancer cells with primary human endothelial cells led to robust
125 endothelial cell labeling (Fig. 3c, d). As anticipated, receiver cell labeling required sGFP-
126 expression on the sender cell and αGFP expression on the receiver cells. Furthermore, co-
127 culturing sGFP-expressing cancer cells with primary cortical neurons expressing αGFP also led
128 to receiver cell labeling (Supplementary Fig. S9c, d). Thus, G-baToN-based labeling extends
129 beyond transformed cell types and can label diverse primary cell types.

130 To further test the generalizability of this system and determine whether primary cells
131 can serve as both sender and receiver cells, we assessed G-baToN-based GFP transfer in the
132 context of two well-established heterotypic cell-cell interactions: endothelial cells with smooth
133 muscle cells and astrocytes with neurons. Consistent with our previous results, we found that
134 sGFP-expressing primary cells (both endothelial cells and astrocytes) were able to transfer GFP
135 to neighboring αGFP-expressing receivers (Fig. 3e, f: smooth muscle cells; Fig. 3g and
136 Supplementary Fig. 9a, b: cortical neurons). Finally, given the importance of adaptive immune
137 cell interactions with cancer cells, we assessed whether the G-baToN could map the interactions
138 of primary human CD4 and CD8 T cells with lung cancer cells (Fig. 3h and Supplementary Fig.
139 10a, b). αGFP-expressing CD4 and CD8 T cells that interacted with sGFP-expressing lung
140 cancer cells were specifically labeled (Fig. 3h and Supplementary Fig. 10a). Inversely, αGFP-
141 expressing cancer cells that interacted with sGFP-expressing CD4 T cells were also specifically
142 identified by G-baToN labeling (Supplementary Fig. 10b).
143 Our data document the ability of diverse primary cell types to serve as both sender and
144 receiver cells, suggesting that baToN systems are not only simple, sensitive and rapid, but also
145 generalizable. Multicolor baToN systems will enable qualitative and quantitative analyses of
146 higher-order interactions. Finally, the ability of baToN systems to co-transfer protein, DNA or
147 chemical cargos suggests that this versatile platform could be leveraged to manipulate target cell
148 functions. The simplicity of this two-component system, combined with its generalizability
149 across cell types, excellent foreground to background, and rapid labeling, should enable facile
150 analysis of cell-cell interaction dynamics and have a broad impact on our ability to understand
151 the outputs of cell-cell interactions across various biological systems.

152

153

154

155 **Figure Legends**

156

157 **Figure 1. GFP-based Touching Nexus (G-baToN) leads to cell-cell interaction-dependent**

158 **receiver cell labeling.**

159 **a.** Schematic of the G-baToN system. Surface GFP (sGFP) on a sender cell is transferred to a

160 receiver cell expressing a cell surface anti-GFP nanobody (αGFP) leading to GFP labeling of the

161 "touched" receiver.

162 **b.** GFP transfer from sGFP-expressing KPT lung cancer sender cells (marked by intracellular

163 tdTomato) to αGFP-expressing 293 receiver cells. Receiver cell labeling is sGFP- and αGFP-

164 dependent. Control sender cells do not express sGFP. Control receiver cells do not express

165 αGFP. Cytoplasmic GFP (Cyto-GFP) is not transferred to receiver cells. Sender and receiver

166 cells were seeded at a 1:1 ratio and co-cultured for 24 hours. Receivers were defined as

167 $Tomato^{neg}PI^{neg}$ cells.

168 **c.** GFP transfer to 293 receiver cells requires direct cell-cell contact. Receiver cells separated

169 from sender cells by a transwell chamber are not labeled. Sender and receiver cells were seeded

170 in upper and lower chambers respectively at a 1:1 ratio and cultured for 24 hours. Receivers were

171 defined as $Tomato^{neg}PI^{neg}$ cells.

172 **d.** GFP transfer to 293 receiver cells requires sGFP-αGFP interaction and is blocked by anti-GFP

173 antibody in a dose-dependent manner. sGFP sender cells were pre-incubated with the indicated

174 concentration of anti-GFP antibody for 2 hours, washed with PBS, and then co-cultured with
175 receiver cells at a 1:1 ratio for 24 hours. Receivers were defined as $Tomato^{neg}PI^{neg}$ cells.
176 **e.** Time-lapse imaging of GFP transfer from a sGFP-expressing sender cell to an αGFP-
177 expressing receiver cell. Time after contact is indicated. Receiver cell is outlined with white
178 dashed line. Scale bar: 10 μm.
179 **f.** Analysis of GFP Mean Fluorescence Intensity (MFI) of αGFP receiver cells (marked by
180 intracellular BFP) co-cultured with sGFP sender cells (marked by intracellular tdTomato) co-
181 cultured for the indicated amount of time. Sender and receiver cells were seeded at a 1:1 ratio.
182 Receivers were defined as $Tomato^{neg}PI^{neg}BFP^{pos}$ cells.
183 **g.** Percentage of labeled αGFP receiver cells after co-culture with different numbers of sender
184 cells for 24 hours. Receivers were defined as $Tomato^{neg}PI^{neg}BFP^{pos}$ cells.
185 **h.** Detection of rare labeled αGFP receiver cells after co-culture with sGFP sender cells at
186 approximately a $1:10^5$ ratio for 24 hours. Receivers were defined as $Tomato^{neg}PI^{neg}BFP^{pos}$ cells.
187
188 **Figure 2. X-baToN systems enable recording of multicellular interactions and cell-cell**
189 **interaction-based cargo transfer.**
190 **a.** Schematic of the AND gate-baToN system. sGFP and smCherry sender cells express either
191 sGFP or mCherry. Dual receiver cells express both αGFP (LaG17, tagged by Myc-tag) and
192 αmCherry (LaM4, tagged by intracellular BFP).
193 **b.** Representative FACS plots of dual receiver 293 cells cultured with the indicated 293 sender
194 cells at 1:1 (for single sender cell) or 1:1:1 (for dual sender cells) ratios. Percent of labeled
195 receiver cells (gated as BFP^{pos}) after 24 hours of co-culture is indicated as mean +/- SD of
196 triplicate cultures.

197 **c.** Diagram of HaloTag-baToN system. Sender cells (marked by intracellular 2A-mCherry)
198 express surface HaloTag-GFP fusion which can be loaded with HaloTag ligands (in this example
199 AF660). Receiver cells express αGFP (LaG17, tagged by intracellular BFP).
200 **d.** Representative plot of GFP and AF660 intensity in αGFP 293 receiver cells co-cultured with
201 HaloTag-GFP KP (lung adenocarcinoma) sender cells at a 1:1 ratio for 6 hours. Receivers were
202 defined as $mCherry^{neg}PI^{neg}BFP^{pos}$ cells.
203 **e.** Diagram of dual color GCN4-HaloTag-baToN system. Sender cells (marked by intracellular
204 2A-mCherry) express surface 4XGCN4 associated with HaloTag, loaded with either AF488- or
205 AF660- conjugated HaloTag ligand. Receiver cells express αGCN4 (tagged by intracellular
206 BFP).
207 **f.** AF488/AF660 GCN4-HaloTag sender ratio in the co-culture directly proportional to
208 AF488/AF660 intensity (MFI) of αGCN4 receiver after 6 hours of co-culture. Receivers were
209 defined as $mCherry^{neg}PI^{neg}BFP^{pos}$ cells.
210 **g.** Diagram of using GCN4-HaloTag sender to transfer ssDNA into αGCN4 receiver cells.
211 Sender cells (marked by intracellular 2A-mCherry) express surface 4XGCN4 associated with
212 HaloTag, loaded with 5' HaloTag ligand, 3' biotin dual conjugated ssDNA (21 nt), then stained
213 with Avidin-AF647. Receiver cells express αGCN4 (tagged by intracellular BFP).
214 **h.** Representative plot of AF647 intensity in αGCN4 293 receiver cells co-cultured with GCN4-
215 HaloTag 293 sender cells at a 1:1 ratio for 6 hours. Receivers were defined as
216 $mCherry^{neg}PI^{neg}BFP^{pos}$ cells.
217
218 **Figure 3. G-baToN is a generalized system that can be used for touching-based labeling**
219 **between various cell types.**

220 **a.** Many different cell lines and primary cell types can serve as receiver cells. Receiver cells
221 expressing αGFP were co-cultured with sGFP-expressing KPT sender cells for 24 hours. MFI of
222 GFP on Tomato^{neg}PI^{neg}BFP^{pos} receiver cells was assessed by FACS analysis and is shown as fold
223 change relative to monocultured receiver cells. For lung epithelial cells and kidney epithelial
224 cells MFI of GFP on Tomato^{neg}PI^{neg}BFP^{pos}EpCAM^{pos} cells is shown as mean +/- SD of triplicate
225 cultures. SkMC: skeletal muscle cells. Astro: Astocytes. Hepato: hepatocytes. Spleno:
226 splenocytes.
227 **b.** Many different cell lines and primary cell types can serve as sender cells. Sender cells
228 expressing sGFP were co-cultured with αGFP 293 receiver cells for 24 hours. MFI of GFP on
229 mCherry^{neg}PI^{neg}BFP^{pos} receiver cells was assessed by flow cytometry and is shown as fold
230 change relative to monocultured 293 receiver cells. Mean +/- SD of triplicate cultures is shown.
231 **c, d.** G-baToN can detect cancer cell-endothelial cell (EC) interactions. HUVECs expressing
232 αGFP were co-cultured with or without Tomato^{pos} sGFP-expressing lung cancer sender cells at a
233 1:1 ratio for 24 hours. MFI of GFP on PI^{neg}Tomato^{neg}BFP^{pos}CD31^{pos} Receiver cells was assessed
234 by flow cytometry and is shown as mean +/- SD of triplicate cultures (**c**). Representative images
235 of Tomato^{pos} sGFP-expressing lung cancer sender cells co-cultured with either control HUVEC
236 receiver cells (HUVECs expressing BFP) or αGFP HUVEC receiver cells at a 1:1 ratio for 24
237 hours (**d**). Scale bars = 50 μm.
238 **e,f.** G-baToN can detect endothelial cell (EC)-smooth muscle cell (SMC) interactions. Primary
239 human umbilical artery smooth muscle cells (HUASMC) expressing αGFP were co-cultured
240 with or without sGFP-expressing HUVEC senders cells at a 1:1 ratio for 24 hours. MFI of GFP
241 on PI^{neg}BFP^{pos} receiver cells was assessed by flow cytometry and is shown as mean +/- SD of
242 triplicate cultures (**e**). Representative images of sGFP-expressing HUVEC sender cells co-

243 cultured with either control HUASMC receiver cells (expressing BFP) or αGFP HUASMC
244 receiver cells at a 1:1 ratio for 24 hours (**d**). Scale bars = 50 μm.
245 **g**. Representative images of sGFP-expressing astrocyte sender cells co-cultured with either
246 control neuron receivers or αGFP neuron receivers at a 1:2 ratio for 24 hours. Neurons were
247 stained with Microtubule Associated Protein 2 (Map2). Scale bars = 50 μm. Higher
248 magnification of the boxed areas are shown on the right.
249 **h.** G-baToN can detect cancer cell-T cell interactions. Primary human $CD4^{pos}$ (left) or $CD8^{pos}$
250 (right) T cells were co-cultured with sGFP-expressing lung cancer sender cells (A549 cells) at a
251 2:1 ratio for 24 hours. Receivers were defined as $mCherry^{neg}Near\text{-}IR^{neg}BFP^{pos}CD4^{pos}/CD8^{pos}$ T
252 cells.
253
254 **Supplementary Figure 1. Features of the synNotch, LIPSTIC, and G-BaToN cell-cell**
255 **interaction reporter systems.**
256 Overview of systems that enable labeling of cells after cell-cell contact.
257
258 **Supplementary Figure 2. GFP transfer requires direct GFP-αGFP interaction.**
259 **a.** GFP protein is transferred to receiver cells. Western blot analysis of FACS purified Control
260 and αGFP receiver 293 cells cultured in isolation or co-culture with sGFP Tomato-positive
261 sender cells (mouse KPT lung cancer cells) for 24 hours. sGFP but not Tomato is present in
262 touched αGFP receiver cells. Human mitochondrial antigen (hu-Mito) is a marker for receiver
263 cells. GAPDH shows loading. Rightmost lane is sGFP sender cells.
264 **b.** GFP cannot be transferred from fixed sGFP sender cells to live αGFP receiver cells. sGFP
265 sender cells were fixed in 1% PFA for 5 minutes and washed with PBS before co-cultured with

266 αGFP receiver cells at a 1:1 ratio for 24 hours. Receivers were defined as Tomato^{neg}PI^{neg}BFP^{pos}
267 cells.
268 **c.** GFP transfer to 293 receiver cells required sGFP-αGFP recognition. GFP is transferred from
269 sGFP sender cells to αGFP-receiver cells but not from sGFP sender cells to αmCherry-receiver
270 cells. Control receiver cells do not express any nanobody. Sender and receiver cells were co-
271 cultured at a 1:1 ratio for 24 hours. Receivers were defined as Tomato^{neg}PI^{neg}BFP^{pos} cells.
272 **d.** GFP transfer to receiver cells is accompanied by a reduction of GFP on the sender cells. GFP
273 expression on sender cells after 24 hour co-culture with control or αGFP-expressing 293 receiver
274 cells at a 1:1 ratio. Co-culture with αGFP expressing but not control receiver cells reduced GFP
275 on sGFP sender cells. Senders were defined as Tomato^{pos}DAPI^{neg}BFP^{neg} cells.
276 **e.** GFP transfer is accompanied with αGFP internalization on receiver cells. Analysis of surface
277 αGFP (Myc-tag) on 293 receiver cell co-cultured for 24 hours with sGFP sender cells. Receivers
278 were defined as Tomato^{neg}PI^{neg} cells.
279 **f.** GFP transfer to 293 receiver cells is partially dependent on membrane dynamics of
280 endocytosis. Both a clathrin inhibitor (Pitstop, 20 μM) and a dynamin inhibitor (Dyngo 4a, 10
281 μM) partially inhibit GFP transfer from sGFP sender cells to αGFP receivers. Inhibitors were
282 present during the 24 hour co-culture. Receivers were defined as Tomato^{neg}PI^{neg} cells.
283 **g.** GFP transfer to αGFP 293 receiver cells can be very rapid. A shift in GFP MFI was detected 5
284 minutes after mixing sGFP sender cells with αGFP receiver cell. Receivers were defined as
285 Tomato^{neg}PI^{neg}BFP^{pos} cells. MFI mean +/- SD of triplicate cultures is shown.
286 **h.** Rapid GFP degradation in touched receiver cells after removal of the sGFP sender cells. After
287 6 hours co-culture, GFP positive receiver cells were purified by FACS followed by culture
288 without sender cells. Receivers were defined as mCherry^{neg}PI^{neg}BFP^{pos} cells. GFP MFI in

289 receiver cells reduced rapidly ($T_{1/2}$ approximately 2 hours). MFI mean +/- SD of triplicate
290 cultures is shown.
291
292 **Supplementary Figure 3. Transmembrane domains and the nanobody affinity impact**
293 **sGFP transfer and receiver cell labeling.**
294 **a.** Schematic of the sender and receiver cells used to determine the impact of different αGFP
295 transmembrane (TM) domains. TM domains contain the TM domain itself as well as membrane
296 proximal regions from the indicated mouse (m) and human (h) proteins.
297 **b.** Different TM domains impact cell surface αGFP expression on 293 receiver cells. Membrane
298 αGFP was accessed by anti-Myc staining. Control receiver cells do not express any nanobody.
299 Mean +/- SD of Myc MFI in triplicate cultures is shown.
300 **c.** VEGFR2 TM domain on αGFP receivers enables highest GFP transfer efficiency. Receiver
301 cells expressing αGFP linked by different TM domains were co-cultured with sGFP sender cells
302 at a 1:1 ratio for 6 hours. Receivers were defined as $Tomato^{neg}PI^{neg}$ cells.
303 **d**. Schematic of the sender and receiver cells used to determine the impact of different sGFP TM
304 domains and different αGFP nanobodies on G-baToN-based labeling. TM domains contain the
305 TM domain itself as well as membrane proximal regions from the indicated mouse (m) and
306 human (h) proteins.
307 **e.** Different nanobodies exhibit different levels of expression on 293 receiver cells. Total αGFP
308 expression was assessed by BFP intensity. Mean +/- SD of GFP MFI in triplicate cultures is
309 shown.
310 **f.** αGFP affinity influences transfer of GFP to touched 293 receiver cells. Receiver cells
311 expressing different αGFP nanobodies were co-cultured with sGFP sender cells at a 1:1 ratio for

312 6 hours. GFP transfer was assessed by flow cytometry. GFP intensity on Tomato^{neg}PI^{neg}BFP^{pos}
313 receiver cells is shown as mean +/- SD of triplicate cultures.
314 **g.** Different TM domains on sGFP impact its expression in 293 sender cells. sGFP expression in
315 sender cells was assessed by flow cytometry for GFP. Mean +/- SD of GFP MFI in triplicate
316 cultures is shown.
317 **h.** PDGFR TM domain on sGFP minimized retrograde transfer of αGFP from receiver cells to
318 293 sGFP sender cells. αGFP transfer to sGFP senders were determined as the percentage of
319 mCherry^{pos}GFP^{pos} sender cells that were also BFP^{pos}. Cells were co-cultured for 6 hours at a 1:1
320 ratio. Mean +/- SD of triplicate cultures is shown.
321
322 **Supplementary Figure 4. X-baToN systems enable fluorescent labeling via various antigen-**
323 **nanobody/scFV pairs.**
324 **a.** Schematic of the surface BFP (sBFP)-baToN system. Sender cell (marked by intracellular
325 tdTomato) expresses sBFP and receiver cell expresses αGFP.
326 **b.** The cross reactivity of αGFP with BFP allow BFP to be transferred from sBFP sender to
327 αGFP receiver cells. sBFP senders and αGFP receivers were co-cultured at 1:1 ratio for 24 hours.
328 Receivers were defined as toTomato^{neg}PI^{neg} cells. BFP MFI of receiver cells is shown as mean
329 +/- SD of triplicate cultures.
330 **c.** Schematic of the surface mCherry (smCherry)-baToN system. Sender cell (marked by
331 intracellular GFP) expresses smCherry and receiver cell expresses αmCherry (tagged by
332 intracellular BFP)
333 **d.** The pairing between mCherry and αmCherry enable mCherry transfer from smCherry 293
334 sender cells to αmCherry-expressing 293 receiver cells. smCherry senders are not able to transfer

335 mCherry to αGFP receiver cells. smCherry sender cells were co-cultured with αGFP or
336 αmCherry receiver cells at a 1:1 ratio for 24 hours. Receivers were defined as $GFP^{neg}BFP^{pos}$
337 cells. mCherry MFI of receiver cell is shown as mean +/- SD of triplicate cultures. smCherry 293
338 sender is not able to transfer mCherry to αGFP 293 receiver.
339 **e.** Schematic of the surface GCN4 (sGCN4)-baToN system. Sender cells (marked by intracellular
340 2A-mCherry) express cell surface 4X GCN4 peptide fused with GFP. Receiver cells express a
341 cell surface anti-GCN4 single-chain variable fragment (scFV; αGCN4, tagged by intracellular
342 BFP).
343 **f.** The pairing between GCN4 and αGCN4 enables co-transfer of GFP from 4X sGCN4-GFP
344 senders to αGCN4 receivers 24 hours after co-culture at a 1:1 ratio. Receivers were defined as
345 $mCherry^{neg}PI^{neg}BFP^{pos}$ cells. GFP MFI of receiver cell is shown as mean +/- SD of triplicate
346 cultures. sGFP sender are not able to transfer GFP to αGCN4 receivers.
347
348 **Supplementary Figure 5. Dual color-baToN systems enable labeling in complex cell-cell**
349 **interaction systems.**
350 **a.** Diagram of the Reciprocal-baToN system. Cell A expresses sGFP and αmCherry (tagged by
351 intracellular BFP), Cell B expresses smCherry and αGFP (tagged by Myc-tag).
352 **b.** Representative FACS plots of cell A and cell B monocultures (left 2 panels) and after co-
353 culture at a 5:1 ratio for 24 hours. Percent of labeled cells is indicated as mean +/- SD of
354 triplicate cultures.
355 **c.** Representative image of reciprocal labeling of cell A and cell B co-cultured for 24 hours. Cells
356 are outlined with a white dashed line. Cell A is BFP and GFP double positive and Cell B is

357 mCherry positive. Touched cell A is BFP, GFP and mCherry triple positive and touched cell B is
358 GFP and mCherry double positive (pointed out by white letter). Scale bar: 10 μm.
359 **d.** Representative image of dual receiver cells co-cultured with indicated sender cells. Cells are
360 outlined with a white dashed line. Dual receiver cells are BFP positive and sender touched dual
361 receiver cells are pointed out by white arrows. Scale bar: 10 μm.
362 **e**. Diagram of the BFP/GFP AND gate-baToN system. sBFP sender cells express intracellular
363 Tomato and surface BFP, sGFP sender cells express intracellular Tomato and surface GFP.
364 Common receiver cells expressed αGFP.
365 **f.** Representative FACS plots of common receiver 293 cells cultured with the indicated
366 $Tomato^{pos}$ sender cells at 1:1 (for single sender cell) or 1:1:1 (for dual sender cells) ratios.
367 Receiver cells were gated as $Tomato^{neg}PI^{neg}$. Percent of labeled common receiver cells after 24
368 hours of co-culture is indicated as mean +/- SD of triplicate cultures.
369
370 **Supplementary Figure 6. Using the G-baToN system to co-transfer cargo protein into**
371 **touched receiver cells.**
372 **a.** Diagram of surface tdTomato-GFP (sGFP-Tom) co-transfer into touched receiver cells.
373 Sender cell expresses sGFP-tdTomato and receiver cell expresses αGFP (tagged by intracellular
374 BFP).
375 **b.** Representative FACS plots of αGFP 293 receiver cells cultured with the indicated sender cells
376 at 1:1 ratio for 24 hours. Percent of GFP/Tomato dual labeled receiver cells is indicated as mean
377 +/- SD of BFP^{pos} cells from triplicate cultures.

378 **c.** Diagram of GFP-PuroR co-transfer system. Sender cell expresses surface GFP associated with
379 PuroR (marked by intracellular tdTomato), receiver cell expresses αGFP (tagged by intracellular
380 BFP). PuroR: Gcn5-related N-acetyltransferase.
381 **d.** 293 Sender cells expressing sGFP-PuroR are only modestly resistant to puromycin treatment.
382 293 cells were transfected with plasmids as indicated. 24 hours after transfection, 293 cells were
383 treated with different doses of puromycin for 24 hours. Cell number was assessed by measuring
384 spectrophotometrically at 570 nm (OD570) after crystal violet staining.
385 **e.** Co-transfer of GFP-PuroR from sGFP-PuroR sender cells to αGFP 293 receiver cells confers
386 puromycin resistance to receiver cells. Control, sGFP or sGFP-PuroR sender cells were co-
387 cultured with αGFP 293 receiver cells for 24 hours at a 4:1 ratio before treatment with
388 different dose of puromycin for 48 hours. tdTomato^{neg}PI^{neg}BFP^{pos} cell numbers were counted via
389 FACS.
390
391 **Supplementary Figure 7. The HaloTag-baToN system enables touching based co-transfer.**
392 **a.** Labeling HaloTag-expressing sender cells with AF660 fluorophore. Representative FACS
393 plots of KP (lung adenocarcinoma) sender cells expressing either sGFP or sGFP-sHaloTag
394 incubated with AF660-conjugated HaloTag ligand for 5 minutes on ice. AF660 specifically
395 labeled sHaloTag-GFP sender cells but not sGFP sender cells.
396 **b.** Representative histogram of GFP and AF660 intensity in αGFP 293 receiver cells cultured
397 with HaloTag-GFP sender cells at a 1:1 ratio for 6 hours (complete experiment results for Figure
398 2d). Receivers were defined as mCherry^{neg}PI^{neg}BFP^{pos} cells.
399 **c.** AF660 transfer to αGFP 293 receiver cell is rapid after cell-cell interaction. AF660 MFI shift
400 was detected after mixing sHalo-GFP senders and αGFP receivers and co-culture for 10 minutes.

401 AF660 MFI shift was more dramatic than GFP. Receivers were defined as
402 mCherry^{neg}PI^{neg}BFP^{pos} cells.
403 **d.** Slower AF660 quenching in touched receiver cells after removing sHalo-GFP senders. After 6
404 hours co-culture, GFP/AF660 positive receiver cells were purified via FACS. Analysis of
405 GFP/AF660 MFI in purified receiver cells showed rapid GFP degradation but slower AF660
406 quenching. Receivers were defined as mCherry^{neg}PI^{neg}BFP^{pos} cells.
407 **e.** Representative FACS plots of αGCN4 receiver cells co-cultured with the indicated sender
408 cells at 1:1 (for single sender cell) or 1:1:1 (for dual sender cells) ratios. Percent of labeled
409 receiver cells (gated as mCherry^{neg}PI^{neg}BFP^{pos}) after 6 hours of co-culture is indicated as mean
410 +/- SD of triplicate cultures.
411 **f.** Loading of sender cells with ssDNA. Representative FACS plots of 293 sender cells
412 expressing either sGCN4 or sGCN4-Halo were loaded with 5' HaloTag-ligand, 3' biotin dual
413 conjugated ssDNA (21nt), then stained with Avidin-AF647. AF647 specifically labeled loaded
414 sGCN4-Halo sender cells but not sGCN4 sender cells.
415 **g.** Representative histogram of AF647 intensity in control or αGCN4 293 receiver cells cultured
416 with sGCN4 or sGCN4-Halo sender cells at a 1:1 ratio for 6 hours (complete experiment results
417 for Figure 2h). Receivers were defined as mCherry^{neg}PI^{neg}BFP^{pos} cells.
418
419 **Supplementary Figure 8. Diverse primary mouse cells expressing sGFP can transfer GFP**
420 **to αGFP 293 receivers.**
421 Different primary sender cells were first sorted based on their cell surface markers, then
422 transduced with lentiviral vectors expressing sGFP before being co-cultured with αGFP 293

423 receiver cells for 24 hours. Percentage of $PI^{neg}mCherry^{neg}BFP^{pos}GFP^{pos}$ receiver cells was
424 assessed by flow cytometry.
425 For each primary sender, approximate $sGFP^{pos}$ sender : αGFP^{pos} receiver ratio is indicated: a.
426 Lung epithelial cells (1:180) (sorted $EpCam^{pos}$ cells from dissociated adult lung); b. Kidney
427 epithelial cells (1:20) (sorted $EpCam^{pos}$ cells from dissociated adult kidney); c. Splenocyte
428 (1:20); d. Cardiomyocyte (1:5) (sorted $Sirpa^{pos}$ cells from dissociated adult heart). Percent of
429 labeled cells is indicated as mean +/- SD of triplicate cultures.
430
431 **Supplementary Figure 9. G-baToN can detect neuron-astrocyte, neuron-cancer cell**
432 **interactions.**
433 **a.** Split channels for Figure 3g. Scale bars = 50 μm.
434 **b.** Quantification of Figure 3g using images from 10 different fields. Each dot represents a field.
435 The bar indicates the mean +/- SD. GFP^{pos} neurons were defined as $Map2^{pos}$ cells with GFP.
436 **c.** Representative image of neuron and cancer cell interactions. Scale bars = 50 μm.
437 **d.** Quantification of supplementary Figure 9c using images from 10 different fields. Each dot
438 represents a field. The bar indicates the mean +/- SD. GFP^{pos} neurons were defined as
439 $Map2^{pos}tdTomato^{neg}$ cells with GFP.
440
441 **Supplementary Figure 10. G-baToN can detect CD4 T cell-A549 cancer cell interactions.**
442 **a.** Representative image of A549 cell and CD4 T cell interactions. Scale bars = 10 μm.
443 **b.** Primary human $CD4^{pos}$ T cells expressing sGFP can transfer GFP to αGFP A549 cells after
444 co-culture at a 1:1 ratio for 24 hours. Receivers were defined as
445 $mCherry^{neg}NearIR^{neg}CD4^{neg}BFP^{pos}$ cells.

446 **ACKNOWLEDGEMENTS**

447 We thank the Stanford Shared FACS and Cell Sciences Imaging Facilities for technical
448 support; A. Orantes for administrative support, N. Kipniss and Y.T. Shue for critical reagents; D.
449 Feldser, J. Sage, Y. Chien, N. Kipniss and members of the Winslow laboratory for helpful
450 comments. R.T. was supported by a Stanford University School of Medicine Dean's Postdoctoral
451 Fellowship and a TRDRP Postdoctoral fellowship (27FT-0044). C.W.M. was supported by the
452 NSF Graduate Research Fellowship Program and an Anne T. and Robert M. Bass Stanford
453 Graduate Fellowship. This work was supported by NIH R01-CA175336 (to M.M.W), NIH R01-
454 CA207133 (to M.M.W) and NIH R01-CA230919 (to M.M.W) and in part by the Stanford
455 Cancer Institute support grant (NIH P30-CA124435), 1S10OD01227601 from the National
456 Center for Research Resources (NCRR) and S10RR027431-01 from National Institutes of Health
457 (NIH).

458

459 **METHODS**

460 *Cells, Plasmids and Reagents:*

461 HEK-293T, B16-F10, A549, H460 and HUVEC cells were originally purchased from ATCC;
462 HUASMC were purchased from PromoCell (C-12500); H82 cells were kindly provided by Julien
463 Sage (Stanford School of Medicine); KP (238N1) and KPT (2985T2) lung adenocarcinoma cells
464 were generated in the Winslow Lab. HEK-293T, 238N1, 2985T2 and B16-F10 cells were
465 cultured in DMEM containing 10% FBS, 100 units/mL penicillin and 100 μg/mL streptomycin.
466 A549, H460 and H82 cells were cultured in RPMI1640 media containing 10% FBS, 100
467 units/mL penicillin and 100 μg/mL streptomycin. HUVECs were cultured in Vascular Cell Basal
468 Medium (ATCC, PCS-100-030) with Endothelial Cell Growth Kit (ATCC, PCS-100-041);

469 HUASMC were cultured in Smooth Muscle Cell Growth Medium 2 (PromoCell, C-22062). All
470 cell lines were confirmed to be mycoplasma negative (MycoAlert Detection Kit, Lonza).
471 Pitstop (ab120687) and Dyngo 4a (ab120689) were purchased from Abcam.
472 All plasmids used in this study are listed in Supplementary Table 1 and will be available on
473 Addgene.
474
475 *Antibodies:*
476 Anti-GFP antibody was purchased from MyBioSource (MBS560494), anti-RFP antibody was
477 purchased from Rockland (600-401-379), anti-human mitochondria antibody was purchased
478 from Abcam (ab92824), anti-GAPDH antibody was purchased from Cell Signaling Technology
479 (5174S)
480
481 *Lentiviral Vector Packaging:*
482 Lentiviral vectors were produced using polyethylenimine (PEI)-based transfection of 293T cells
483 with the plasmids indicated in Supplementary Table 1, along with delta8.2 and VSV-G
484 packaging plasmids in 150-mm cell culture plates. Sodium butyrate (Sigma Aldrich, B5887) was
485 added 8 hours after transfection to achieve a final concentration of 20 mM. Medium was
486 refreshed 24 hours after transfection. 20 mL of virus-containing supernatant was collected 36,
487 48, and 60 hours after transfection. The three collections were then pooled and concentrated by
488 ultracentrifugation (25,000 rpm for 1.5 hours), resuspended overnight in 100 μL PBS, then
489 frozen at -80°C.
490
491 *Generation of Stable Cell Lines*

492 Parental cells were seeded at 50% confluency in a 6-well plate the day before transduction (day
493 0). The cell culture medium was replaced with 2 mL fresh medium containing 8 µg/mL
494 hexadimethrine bromide (Sigma Aldrich, H9268-5G), 20 µL ViralPlus Transduction Enhancer
495 (Applied Biological Materials Inc., G698) and 40 µL concentrated lentivirus and cultured
496 overnight (Day 1). The medium was then replaced with complete medium and cultured for
497 another 24 hours (Day 2). Cells were transferred into a 100 mm cell culture dish with appropriate
498 amounts of puromycin (Dose used: 293T: 2 µg/mL; 238N1: 3 µg/mL; 2985T2: 2 µg/mL) and
499 selected for 48 hours (Day 3). After selection, FACS analysis was performed using fluorescent
500 markers indicated in Supplementary Table 2 for validation of selection efficiency.
501
502 *Transwell Co-culture Assay*
503 The Corning® Transwell® polycarbonate membrane cell culture inserts were purchased from
504 Corning Inc (3422 : CS, Corning, NY). sGFP sender cells were seeded in the upper chamber
505 inserts of the transwell (1×10^5/insert). The inserts were then placed back into the plate pre-
506 seeded with 1×10^5/well αGFP receiver cells and cultured in a humidified incubator at 37 °C,
507 with 5% CO_2 for 24 hours. sGFP sender and αGFP receiver cells co-cultured in the same plate
508 under the same conditions were used as control. After 24 hours, the upper chamber inserts were
509 removed, cells in the lower chamber were trypsinized and analyzed by flow cytometry.
510
511 *Live and Fixed Cell Imaging*
512 For live cell microscopy, 2×10^4 sGFP sender and 2×10^4 αGFP receiver cells were seeded into
513 35-mm FluoroDish Cell Culture Dishes (World Precision Instruments, FD35-100) and
514 immediately imaged under a DeltaVision OMX (GE Healthcare) microscope with a 60x oil

515 objective lens (Olympus) in a humidified chamber at 37 °C with 5% CO_2. One image was taken
516 per minute for three hours. Images were collected with a cooled back-thinned EM-CCD camera
517 (Evolve; Photometrics).
518
519 For fixed cell microscopy, sender and receiver cells were seeded at the ratios indicated in
520 Supplementary Table 2 with a total number of 1×10^5 cells onto Neuvitro coated cover slips
521 (Thermo Fisher Scientific, NC0301187) in a 12-well cell culture plate. 24 hours after co-culture,
522 cells were fixed in 4% paraformaldehyde (PFA) PBS solution at room temperature for 10
523 minutes and washed with PBS and distilled water three times each, before mounting onto slides
524 using 50% glycerol. Images were captured using a Leica DMI6000B inverted microscope with
525 an 40x oil objective lens. For quantification, GFP-containing receiver cells were counted.
526 Multiple coverslips were analyzed across independent experiments (n=10).
527
528 *Western Blot*
529 5×10^6 sGFP sender and 5×10^6 αGFP receiver cells were co-cultured in a 100mm cell culture dish
530 for 24 hours. Cells were trypsinized, resuspended in FACS buffer containing propidium iodide
531 (PI) (PBS, 2% FBS, 1 mM EDTA, and 1.5 μM PI). $tdTomato^{neg}PI^{neg}$ cells were sorted and lysed
532 in RIPA buffer (50 mM Tris-HCl (pH 7.4), 150 mM NaCl, 1% Nonidet P-40, and 0.1% SDS)
533 and incubated at 4 °C with continuous rotation for 30 minutes, followed by centrifugation at
534 12,000 × rcf for 10 minutes. The supernatant was collected, and the protein concentration was
535 determined by BCA assay (Thermo Fisher Scientific, 23250). Protein extracts (20–50 μg) were
536 dissolved in 10% SDS-PAGE and transferred onto PVDF membranes. The membranes were
537 blocked with 5% non-fat milk in TBS with 0.1% Tween 20 (TBST) at room temperature for one

538 hour, followed by incubation with primary antibodies diluted in TBST (1:1000 for anti-GFP,
539 anti-Tomato (RFP) and anti-human mitochondria (hu-Mito), 1:5000 for anti-GAPDH) at 4 °C
540 overnight. After three 10-minutes washes with TBST, the membranes were incubated with the
541 appropriate secondary antibody conjugated to HRP diluted in TBST (1:10000) at room
542 temperature for 1 hour. After three 10-minutes washes with TBST, Protein expression was
543 quantified with enhanced chemiluminescence reagents (Fisher Scientific, PI80196).
544
545 *GFP/AF660 Stability*
546 To assess the stability of GFP and AF660 in touched receiver cells, 1×10^7 sGFP or sHalo-GFP
547 sender cells were co-cultured with 1×10^7 αGFP receiver cells in a 150mm cell culture dish for 6
548 hours. Cells were then trypsinized and resuspended in FACS buffer containing propidium iodide.
549 $mCherry^{neg}PI^{neg}BFP^{pos}$ cells were sorted and 1×10^5 cells were re-plated in 12-well plate and
550 cultured for 2, 4, 6, 8, 12, 24 and 48 hours in DMEM containing 10% FBS, 100 units/mL
551 penicillin and 100 µg/mL streptomycin. GFP or AF660 intensity was assessed via FACS analysis
552 of $mCherry^{neg}PI^{neg}BFP^{pos}$ cells and shown as Mean +/- SD of GFP/AF660 MFI in triplicate
553 cultures.
554
555 *Puromycin Resistant Protein Transfer Assay*
556 To validate puromycin resistant protein (GCN5-Related N-Acetyltransferases, PuroR) function
557 in sender cells, 5×10^6 HEK-293T cells were transfected with sGFP-PuroR-PDGFR, sGFP-
558 PDGFR or sGFP-PDGFR-IRES-PuroR in a 100-mm cell culture dish for 12 hours before re-
559 plating into a 12-well plate (1×10^5 cells/well). 24 hours after transfection, cells were treated with
560 1, 2 or 5 µg/mL puromycin for 24 hours. After treatment, dead cells were washed away, and

561 viable cells were fixed by 4% PFA and stained with crystal violet. Stained cells were washed
562 with distilled water three times before extraction with 500 µL of methanol for 15 minutes on a
563 rocker. The absorbance was measured at 570 nm with a spectrophotometer.
564 To count the number of viable receiver cells co-cultured with sGFP-PuroR sender cells, 2×10^5
565 αGFP receiver cells were co-cultured with 8×10^5 sGFP or sGFP-PuroR sender cells in a 6-well
566 plate. 24 hours after co-culture, cells were treated with 2 µg/mL puromycin for 48 hours. Viable
567 $tdTomato^{neg}PI^{neg}BFP^{pos}$ receiver cells were counted via FACS.
568
569 *Primary Mouse Cell Isolation*
570 Mouse (C57BL/6J, The Jackson Laboratory) lung, kidney, heart, hindlimb skeleton muscle,
571 spleen and liver tissue were dissected, cut into small pieces and digested in 5 mL tissue digest
572 media (3.5 mL HBSS-Ca2+ free, 0.5 mL Trypsin-EDTA (0.25%), 5mg Collagenase IV
573 (Worthington), 25 U Dispase (Corning) for 30 minutes in hybridization chamber at 37˚C with
574 rotation. Digestion is then neutralized by adding 5 mL ice cold Quench Solution (4.5 mL L15
575 media, 0.5 mL FBS, 94 µg DNase). Single cell suspensions were generated by filtering through a
576 40uM cell strainer, spinning down at 500 rcf for 5 minutes and washed with PBS twice
577 For primary mouse lung epithelial cells, kidney epithelial cells and cardiomyocyte isolation and
578 culture, the single cell pellets were resuspended in 1mL FACS buffer containing 1:300 dilution
579 of anti-EpCam-AF467 (Biolegend, 118211) (for lung and kidney epithelial cell) or anti-Sirpa-
580 AF467 (Biolegend, 144027) (for cardiomyocyte) antibody and incubated on ice for 20 minutes
581 before FACS sorting. $DAPI^{neg}EpCam^{pos}$ or $DAPI^{neg}Sirpa^{pos}$ cells were sorted and seeded onto a
582 100 mm culture dish precoated with 5 µg/cm2 Bovine Plasma Fibronectin (ScienCell, 8248).

583 For primary skeleton muscle cell, splenocyte and hepatocyte culture, the single cell pellets were
584 resuspended in DMEM containing 20% FBS, 200 units/mL penicillin and 200 µg/mL
585 streptomycin, amphotericin and cultured in 100-mm culture dish at 37°C for 1 hour to remove
586 fibroblast cells. The supernatant containing primary skeletal muscle cells, splenocytes and
587 hepatocytes was then transferred into a new 100-mm culture dish precoated with 5 µg/cm2
588 Bovine Plasma Fibronectin (ScienCell, 8248).
589
590 *Conjugation of HaloTag Ligand to Oligonucleotides*
591 Oligonucleotides to be conjugated with the HaloTag ligand were synthesized with a 5' amino
592 modifier C12 and a 3' biotin group (IDT). Oligonucleotides were initially ethanol-precipitated
593 and subsequently resuspended to 1 mM in conjugation buffer (100 mM Na2HPO4 (Sigma-
594 Aldrich S9763), 150 mM NaCl (Thermo Fisher Scientific S271), pH 8.5). Resuspended oligos
595 were combined with an equal volume of the HaloTag ligand succinimidyl ester (O4) (Promega
596 P6751) resuspended in N,N- dimethylformamide (Sigma-Aldrich D4551) with a 30-fold molar
597 excess of the ligand. Conjugation reactions were conducted overnight at room temperature with
598 constant agitation prior to final cleanup via ethanol precipitation.
599
600 *Loading of HaloTag-Expressing Sender Cells*
601 Prior to loading with HaloTag-conjugated elements, sender cells were washed once in cold PBS
602 following detachment and subsequently resuspended in cold Cell Staining Buffer (BioLegend
603 42021). For loading of HaloTag-conjugated fluorophores, senders were stained at a density of
604 1.00E+07 cells/mL on ice for five minutes in the presence of either 1 µM HaloTag-Alexa Fluor
605 488 (Promega G1001) or 3.5 µM HaloTag-Alexa Fluor 660 (Promega G8471). Stained sender

606 cells were then washed twice in Cell Staining Buffer (500 rcf for 5 min at 4˚C) prior to
607 resuspension in growth media in preparation for co-culture.
608 For loading with HaloTag-conjugated oligonucleotides, sender cells were initially resuspended
609 and incubated with 100 µg/mL salmon sperm DNA (Thermo Fisher Scientific 15632011).
610 Sender cells were then incubated with 3.5 µM HaloTag-conjugated oligonucleotides
611 (5AmMC12/TCTAGGCGCCCGGAATTAGAT/3Bio) and subsequently washed once.
612 Oligonucleotide-loaded sender cells were then stained with 5 µg/mL streptavidin-conjugated
613 Alexa Fluor 647 (Thermo Fisher Scientific S32357) for 30 minutes on ice. The loaded, stained
614 senders were then washed twice and resuspended in growth media in preparation for co-culture.
615
616 *Primary Neuron and Astrocyte Cultures*
617 Primary cortical neurons were dissociated from mouse (C57BL/6J, The Jackson Laboratory)
618 E16.5 embryonic cortices into single cell suspensions with a papain dissociation system
619 (Worthington Biochemical Corporation). Tissue culture plates were coated with poly-L-lysine
620 (0.1% w/v) before seeding cells. Neurons were grown in Neurobasal media (Gibco)
621 supplemented with B-27 serum free supplement (Gibco), GlutaMAX (Gibco), and penicillin-
622 streptomycin (Gibco) in a humidified incubator at 37 °C, with 5% CO2. Half media changes
623 were performed every 4-5 days. Primary astrocytes were dissociated from P0-P1 mouse cortices
624 using the same papain dissociation methods as neurons, except the single cell suspensions were
625 then plated onto tissue culture plates without poly-L-lysine in DMEM with 10% FBS and
626 penicillin-streptomycin. Primary astrocyte cultures were passaged using Accutase (Stemcell
627 Technologies).
628

629 *Primary Human T Cell Cultures*

630 Blood from healthy donors collected in leukoreduction system (LRS) chambers was separated by
631 Ficoll-Paque density gradient to obtain peripheral blood mononuclear cells (PBMCs). $CD4^{pos}$
632 and $CD8^{pos}$ T cells were isolated by negative selection using EasySep Human CD4+ T Cell
633 Isolation Kit and EasySep Human CD8+ T Cell Isolation Kit (STEMCELL Technologies),
634 respectively, according to the manufacturer's instructions. T cells were cultured for 3 days with
635 CD3/CD28 Dynabeads (ThermoFisher Scientific) with 40 IU/mL IL-2 and spinoculated with
636 lentivirus for 2 hours at 400 rcf in the presence of 8 µg/mL polybrene. T cells were expanded
637 following transduction for two days in the presence of CD3/CD28 Dynabeads and 300 IU/mL
638 IL-2 prior to use in assays. Transduced or untransduced $CD4^{pos}$ or $CD8^{pos}$ T cells were co-
639 cultured for 24 hours together with A549 cells. Following co-culture, cells were harvested,
640 stained with antibodies against CD45, CD4, or CD8 (BioLegend) and analyzed on a
641 LSRFortessa flow cytometer (BD Biosciences). Each condition was run in triplicate, and two
642 independent experiments were conducted using T cells from different donors. For microscopy,
643 A549 cells were co-cultured with $CD4^{pos}$ T cells in glass-bottom plates (MatTek Corporation)
644 and imaged on an LSM 700 confocal microscope (Zeiss).

645
646
647
648
649
650
651
652
653
654
655
656
657
658

659 **REFERENCES**

660 1. Zhang, Y. & Liu, F. Multidimensional Single-Cell Analyses in Organ Development and
661 Maintenance. *Trends in cell biology* (2019).
662 2. Tsioris, K., Torres, A.J., Douce, T.B. & Love, J.C. A new toolbox for assessing single cells.
663 *Annual review of chemical and biomolecular engineering* **5**, 455-477 (2014).
664 3. Zhong, S. et al. A single-cell RNA-seq survey of the developmental landscape of the
665 human prefrontal cortex. *Nature* **555**, 524 (2018).
666 4. Zhou, F. et al. Reconstituting the transcriptome and DNA methylome landscapes of
667 human implantation. *Nature* **572**, 660-664 (2019).
668 5. Boisset, J.-C. et al. Mapping the physical network of cellular interactions. *Nature*
669 *methods* **15**, 547-553 (2018).
670 6. Morsut, L. et al. Engineering customized cell sensing and response behaviors using
671 synthetic notch receptors. *Cell* **164**, 780-791 (2016).
672 7. Pasqual, G. et al. Monitoring T cell–dendritic cell interactions in vivo by intercellular
673 enzymatic labelling. *Nature* **553**, 496 (2018).
674 8. Ovcinnikovs, V. et al. CTLA-4–mediated transendocytosis of costimulatory molecules
675 primarily targets migratory dendritic cells. *Science immunology* **4**, eaaw0902 (2019).
676 9. Langridge, P.D. & Struhl, G. Epsin-dependent ligand endocytosis activates Notch by
677 force. *Cell* **171**, 1383-1396. e1312 (2017).
678 10. Li, G. et al. T cell antigen discovery via trogocytosis. *Nature methods* **16**, 183 (2019).
679 11. Fridy, P.C. et al. A robust pipeline for rapid production of versatile nanobody
680 repertoires. *Nature methods* **11**, 1253 (2014).
681 12. Lim, K.H., Huang, H., Pralle, A. & Park, S. Stable, high-affinity streptavidin monomer for
682 protein labeling and monovalent biotin detection. *Biotechnology and bioengineering*
683 **110**, 57-67 (2013).
684 13. Tanenbaum, M.E., Gilbert, L.A., Qi, L.S., Weissman, J.S. & Vale, R.D. A protein-tagging
685 system for signal amplification in gene expression and fluorescence imaging. *Cell* **159**,
686 635-646 (2014).
687 14. Los, G.V. et al. HaloTag: a novel protein labeling technology for cell imaging and protein
688 analysis. *ACS chemical biology* **3**, 373-382 (2008).

689

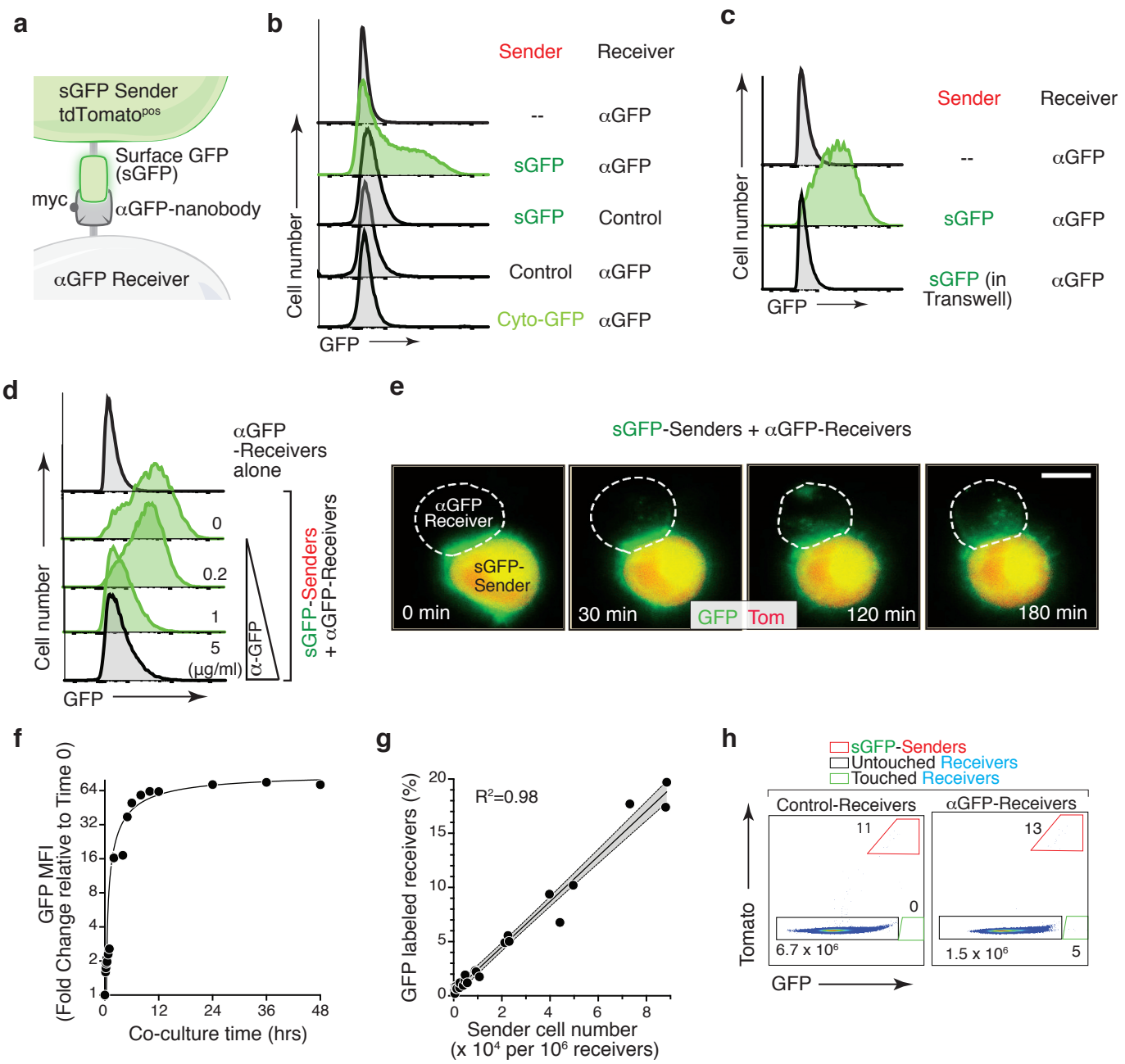

Figure 1. GFP-based Touching Nexus (G-baToN) leads to cell-cell interaction-dependent receiver cell labeling

a. Schematic of the G-baToN system. Surface GFP (sGFP) on a sender cell is transferred to a receiver cell expressing a cell surface anti-GFP nanobody (αGFP) leading to GFP labeling of the "touched" receiver.

b. GFP transfer from sGFP-expressing KPT lung cancer sender cells (marked by intracellular tdTomato) to αGFP-expressing 293 receiver cells. Receiver cell labeling is sGFP- and αGFP- dependent. Control sender cells do not express sGFP. Control receiver cells do not express αGFP. Cytoplasmic GFP (Cyto-GFP) is not transferred to receiver cells. Sender and receiver cells were seeded at a 1:1 ratio and co-cultured for 24 hours. Receivers were defined as Tomato^{neg}PI^{neg} cells.

c. GFP transfer to 293 receiver cells requires direct cell-cell contact. Receiver cells separated from sender cells by a transwell chamber are not labeled. Sender and receiver cells were seeded in upper and lower chambers respectively at a 1:1 ratio and cultured for 24 hours. Receivers were defined as Tomato^{neg}PI^{neg} cells.

d. GFP transfer to 293 receiver cells requires sGFP-αGFP interaction and is blocked by anti-GFP antibody in a dose-dependent manner. sGFP sender cells were pre-incubated with the indicated concentration of anti-GFP antibody for 2 hours, washed with PBS, and then co-cultured with receiver cells at a 1:1 ratio for 24 hours. Receivers were defined as Tomato^{neg}PI^{neg} cells.

e. Time-lapse imaging of GFP transfer from a sGFP-expressing sender cell to an αGFP-expressing receiver cell. Time after contact is indicated. Receiver cell is outlined with white dashed line. Scale bar: 10 μm.

f. Analysis of GFP Mean Fluorescence Intensity (MFI) of αGFP receiver cells (marked by intracellular BFP) co-cultured with sGFP sender cells (marked by intracellular tdTomato) co-cultured for the indicated amount of time. Sender and receiver cells were seeded at a 1:1 ratio. Receivers were defined as Tomato^{neg}PI^{neg}BFP^{pos} cells.

g. Percentage of labeled αGFP receiver cells after co-culture with different numbers of sender cells for 24 hours. Receivers were defined as Tomato^{neg}PI^{neg}BFP^{pos} cells.

h. Detection of rare labeled αGFP receiver cells after co-culture with sGFP sender cells at approximately a 1:10^5 ratio for 24 hours. Receivers were defined as Tomato^{neg}PI^{neg}BFP^{pos} cells.

	synNotch (Morsut *et al.*, Cell, 2016)	**LIPSTIC** (Pasqual *et al.*, Nature, 2018)	**G-baToN** (This manuscript)
Cell-cell interaction	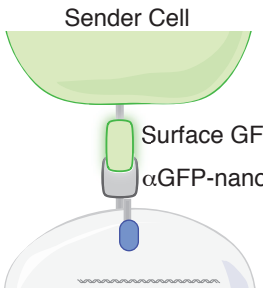	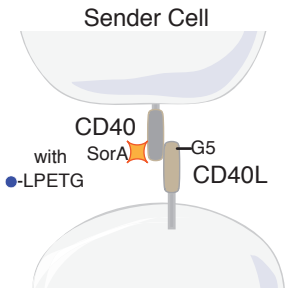	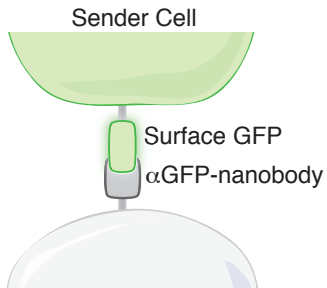
Receiver Cell after interaction	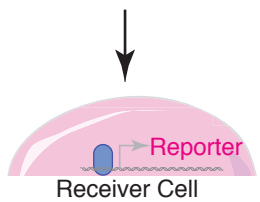	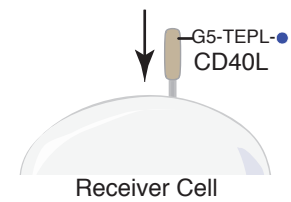	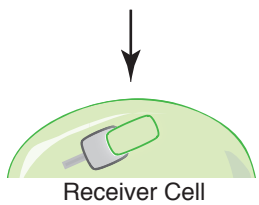
Basis of the labeling	Notch intracellular cleavage leads to transcription factor release and activation of a reporter	Covalent labeling of receptor by ligand associated enzyme	Ligand internalization
Additional requirement for labeling	Engineered reporter in receiver cells	Labeling substrate	None
Determinants of label half-life after touching	Transcription factor half-life and reporter mRNA and protein half-life in the receiver cell	Labeled protein half-life on the receiver cell	Half-life of transferred protein or fluorophore in the receiver cell
Advantages	Generic sender and receivers Generalizable across cell type Compatable with AND gates Tf can drive expression of many genes of interest	Requirement for exogenous substrate adds temporal control of labelling Conceptually generalizable to other receptor ligand pairs	Simple two-component system Low background Single cell level sensitivity Generalizable across cell type Generic sender and receivers Complex cell-cell interactions
Potential disadvantages	Engineered ligand-receptor interactions could influence cell-cell contact Background activation or reporter could be leaky	Requires knowledge of receptor-ligand interactions between cell types of interest	Engineered ligand-receptor interactions could influence cell-cell contact

Supplementary Figure 1. Features of the synNotch, LIPSTIC, and G-BaToN cell-cell interaction reporter systems.
Overview of systems that enable labeling of cells after cell-cell contact.

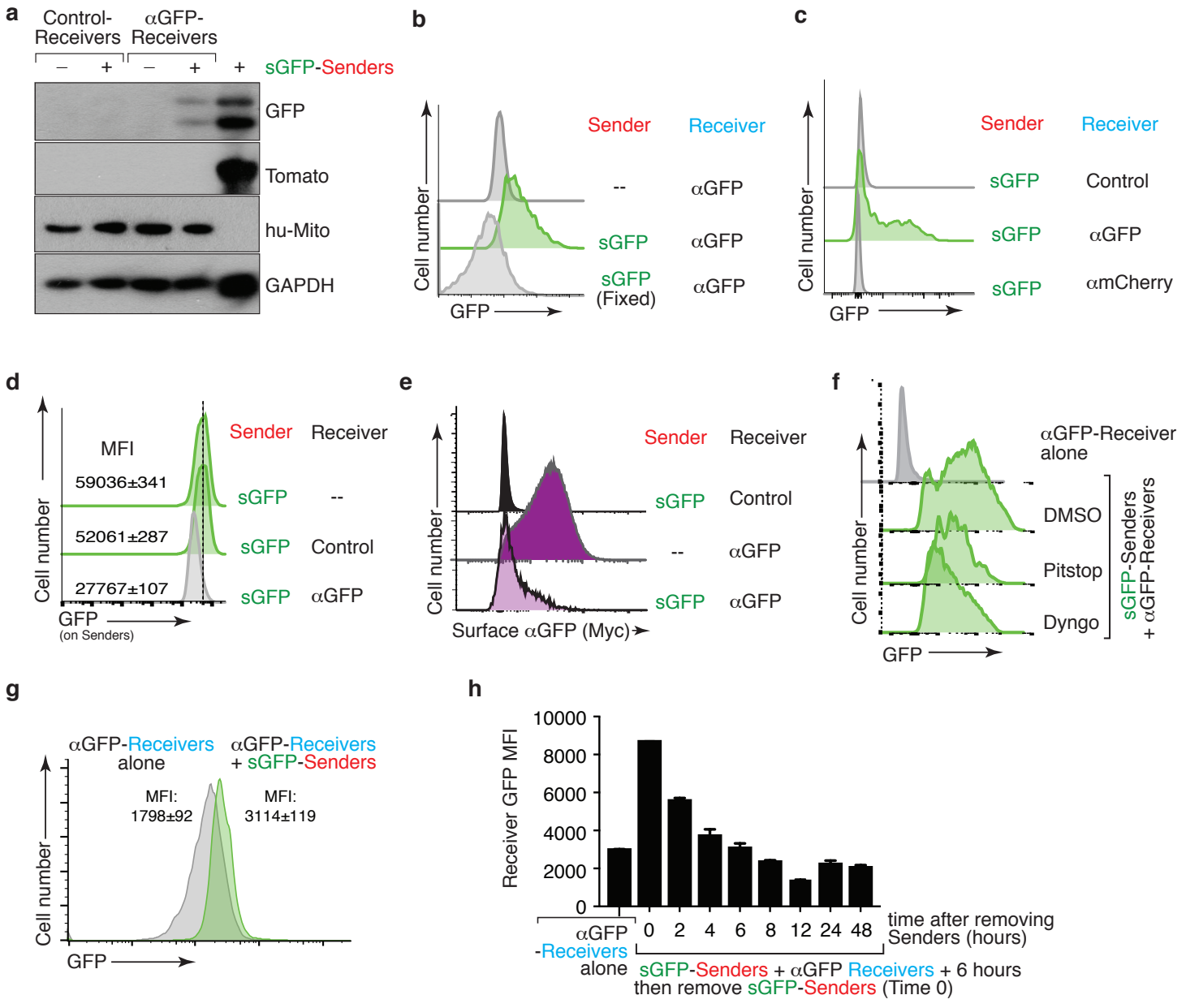

Supplementary Figure 2. GFP transfer requires direct GFP-αGFP interaction.

a. GFP protein is transferred to receiver cells. Western blot analysis of FACS purified Control and αGFP receiver 293 cells cultured in isolation or co-culture with sGFP Tomato-positive sender cells (mouse KPT lung cancer cells) for 24 hours. sGFP but not Tomato is present in touched αGFP receiver cells. Human mitochondrial antigen (hu-Mito) is a marker for receiver cells. GAPDH shows loading. Rightmost lane is sGFP sender cells.

b. GFP cannot be transferred from fixed sGFP sender cells to live αGFP receiver cells. sGFP sender cells were fixed in 1% PFA for 5 minutes and washed with PBS before co-cultured with αGFP receiver cells at a 1:1 ratio for 24 hours. Receivers were defined as $Tomato^{neg}PI^{neg}BFP^{pos}$ cells.

c. GFP transfer to 293 receiver cells required sGFP-αGFP recognition. GFP is transferred from sGFP sender cells to αGFP-receiver cells but not from sGFP sender cells to αmCherry-receiver cells. Control receiver cells do not express any nanobody. Sender and receiver cells were co-cultured at a 1:1 ratio for 24 hours. Receivers were defined as $Tomato^{neg}PI^{neg}BFP^{pos}$ cells.

d. GFP transfer to receiver cells is accompanied by a reduction of GFP on the sender cells. GFP expression on sender cells after 24 hour co-culture with control or αGFP-expressing 293 receiver cells at a 1:1 ratio. Co-culture with αGFP expressing but not control receiver cells reduced GFP on sGFP sender cells. Senders were defined as $Tomato^{pos}DAPI^{neg}BFP^{neg}$ cells.

e. GFP transfer is accompanied with αGFP internalization on receiver cells. Analysis of surface αGFP (Myc-tag) on 293 receiver cell co-cultured for 24 hours with sGFP sender cells. Receivers were defined as $Tomato^{neg}PI^{neg}$ cells.

f. GFP transfer to 293 receiver cells is partially dependent on membrane dynamics of endocytosis. Both a clathrin inhibitor (Pitstop, 20 μM) and a dynamin inhibitor (Dyngo 4a, 10 μM) partially inhibit GFP transfer from sGFP sender cells to αGFP receivers. Inhibitors were present during the 24 hour co-culture. Receivers were defined as $Tomato^{neg}PI^{neg}$ cells.

g. GFP transfer to αGFP 293 receiver cells can be very rapid. A shift in GFP MFI was detected 5 minutes after mixing sGFP sender cells with αGFP receiver cell. Receivers were defined as $Tomato^{neg}PI^{neg}BFP^{pos}$ cells. MFI mean +/- SD of triplicate cultures is shown.

h. Rapid GFP degradation in touched receiver cells after removal of the sGFP sender cells. After 6 hours co-culture, GFP positive receiver cells were purified by FACS followed by culture without sender cells. Receivers were defined as $mCherry^{neg}PI^{neg}BFP^{pos}$ cells. GFP MFI in receiver cells reduced rapidly ($T_{1/2}$ approximately 2 hours). MFI mean +/- SD of triplicate cultures is shown.

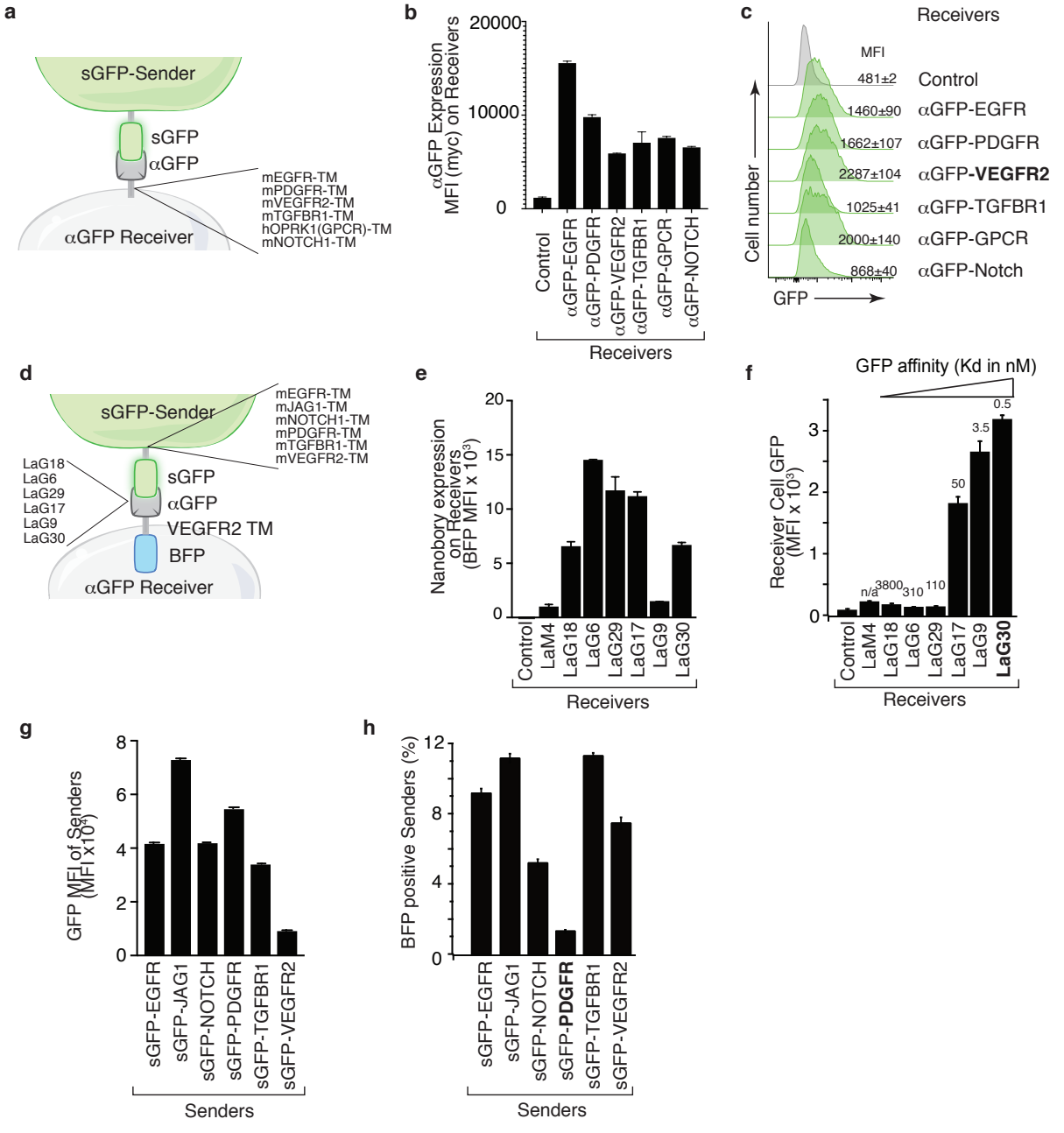

Supplementary Figure 3. Transmembrane domains and the nanobody affinity impact sGFP transfer and receiver cell labeling.

a. Schematic of the sender and receiver cells used to determine the impact of different αGFP transmembrane (TM) domains. TM domains contain the TM domain itself as well as membrane proximal regions from the indicated mouse (m) and human (h) proteins.

b. Different TM domains impact cell surface αGFP expression on 293 receiver cells. Membrane αGFP was accessed by anti-Myc staining. Control receiver cells do not express any nanobody. Mean +/- SD of Myc MFI in triplicate cultures is shown.

c. VEGFR2 TM domain on αGFP receivers enables highest GFP transfer efficiency. Receiver cells expressing αGFP linked by different TM domains were co-cultured with sGFP sender cells at a 1:1 ratio for 6 hours. Receivers were defined as Tomato^{neg}PI^{neg} cells.

d. Schematic of the sender and receiver cells used to determine the impact of different sGFP TM domains and different αGFP nanobodies on G-baTon-based labeling. TM domains contain the TM domain itself as well as membrane proximal regions from the indicated mouse (m) and human (h) proteins.

e. Different nanobodies exhibit different levels of expression on 293 receiver cells. Total αGFP expression was assessed by BFP intensity. Mean +/- SD of GFP MFI in triplicate cultures is shown.

f. αGFP affinity influences transfer of GFP to touched 293 receiver cells. Receiver cells expressing different αGFP nanobodies were co-cultured with sGFP sender cells at a 1:1 ratio for 6 hours. GFP transfer was assessed by flow cytometry. GFP intensity on Tomato^{neg}PI^{neg}BFP^{pos} receiver cells is shown as mean +/- SD of triplicate cultures.

g. Different TM domains on sGFP impact its expression in 293 sender cells. sGFP expression in sender cells was assessed by flow cytometry for GFP. Mean +/- SD of GFP MFI in triplicate cultures is shown.

h. PDGFR TM domain on sGFP minimized retrograde transfer of αGFP from receiver cells to 293 sGFP sender cells. αGFP transfer to sGFP senders were determined as the percentage of mCherry^{pos}GFP^{pos} sender cells that were also BFP^{pos}. Cells were co-cultured for 6 hours at a 1:1 ratio. Mean +/- SD of triplicate cultures is shown.

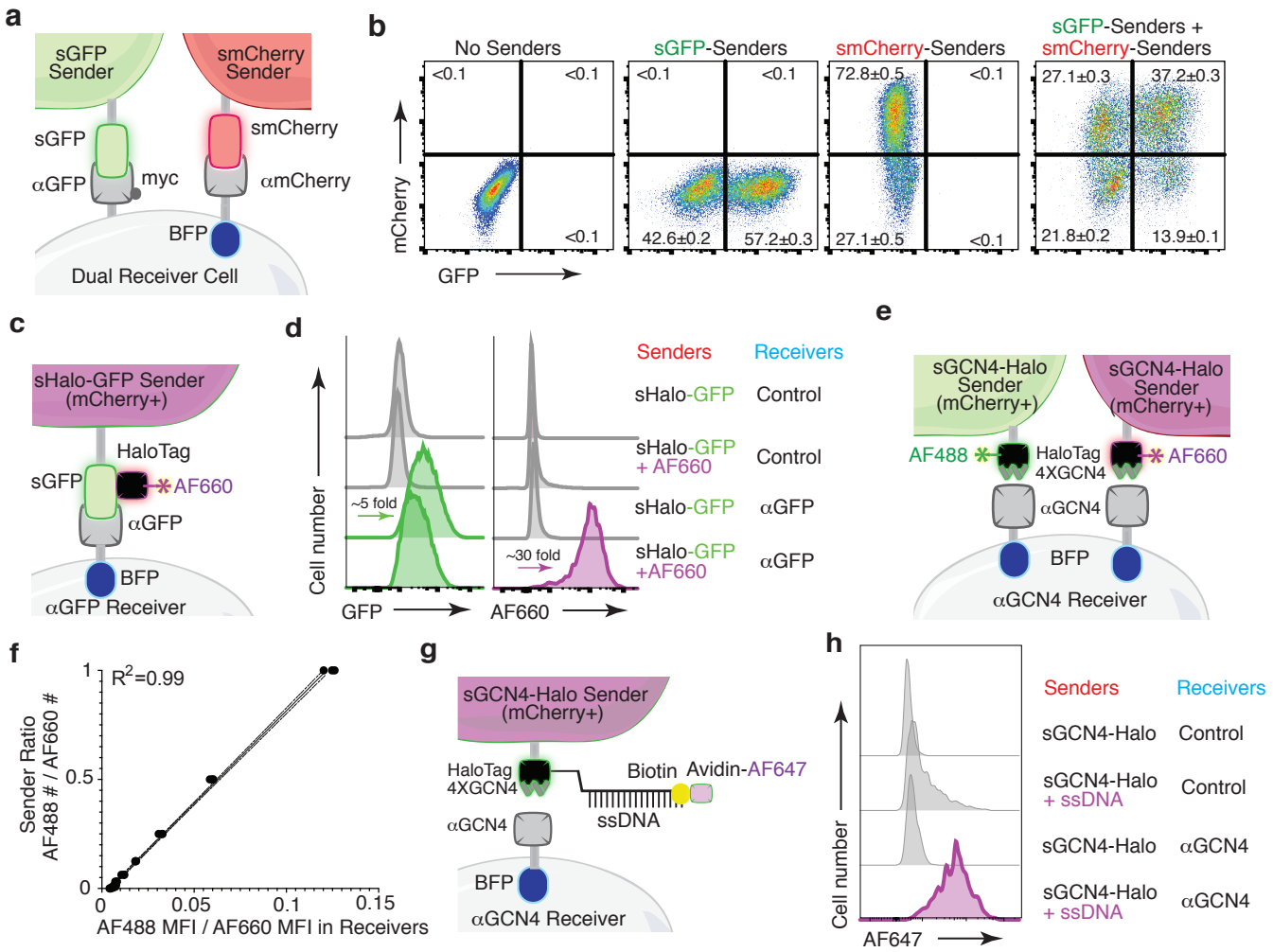

Figure 2. X-baToN systems enable recording of multicellular interactions and cell-cell interaction-based cargo transfer.
a. Schematic of the AND gate-baToN system. sGFP and smCherry sender cells express either sGFP or mCherry. Dual receiver cells express both αGFP (LaG17, tagged by Myc-tag) and αmCherry (LaM4, tagged by intracellular BFP).
b. Representative FACS plots of dual receiver 293 cells cultured with the indicated 293 sender cells at 1:1 (for single sender cell) or 1:1:1 (for dual sender cells) ratios. Percent of labeled receiver cells (gated as BFP^{pos}) after 24 hours of co-culture is indicated as mean +/- SD of triplicate cultures.
c. Diagram of HaloTag-baToN system. Sender cells (marked by intracellular 2A-mCherry) express surface HaloTag-GFP fusion which can be loaded with HaloTag ligands (in this example AF660). Receiver cells express αGFP (LaG17, tagged by intracellular BFP).
d. Representative plot of GFP and AF660 intensity in αGFP 293 receiver cells co-cultured with HaloTag-GFP KP (lung adenocarcinoma) sender cells at a 1:1 ratio for 6 hours. Receivers were defined as $mCherry^{neg}PI^{neg}BFP^{pos}$ cells.
e. Diagram of dual color GCN4-HaloTag-baToN system. Sender cells (marked by intracellular 2A-mCherry) express surface 4XGCN4 associated with HaloTag, loaded with either AF488- or AF660- conjugated HaloTag ligand. Receiver cells express αGCN4 (tagged by intracellular BFP).
f. AF488/AF660 GCN4-HaloTag sender ratio in the co-culture directly proportional to AF488/AF660 intensity (MFI) of αGCN4 receiver after 6 hours of co-culture. Receivers were defined as $mCherry^{neg}PI^{neg}BFP^{pos}$ cells.
g. Diagram of using GCN4-HaloTag sender to transfer ssDNA into αGCN4 receiver cells. Sender cells (marked by intracellular 2A-mCherry) express surface 4XGCN4 associated with HaloTag, loaded with 5' HaloTag ligand, 3' biotin dual conjugated ssDNA (21 nt), then stained with Avidin-AF647. Receiver cells express αGCN4 (tagged by intracellular BFP).
h. Representative plot of AF647 intensity in αGCN4 293 receiver cells co-cultured with GCN4-HaloTag 293 sender cells at a 1:1 ratio for 6 hours. Receivers were defined as $mCherry^{neg}PI^{neg}BFP^{pos}$ cells.

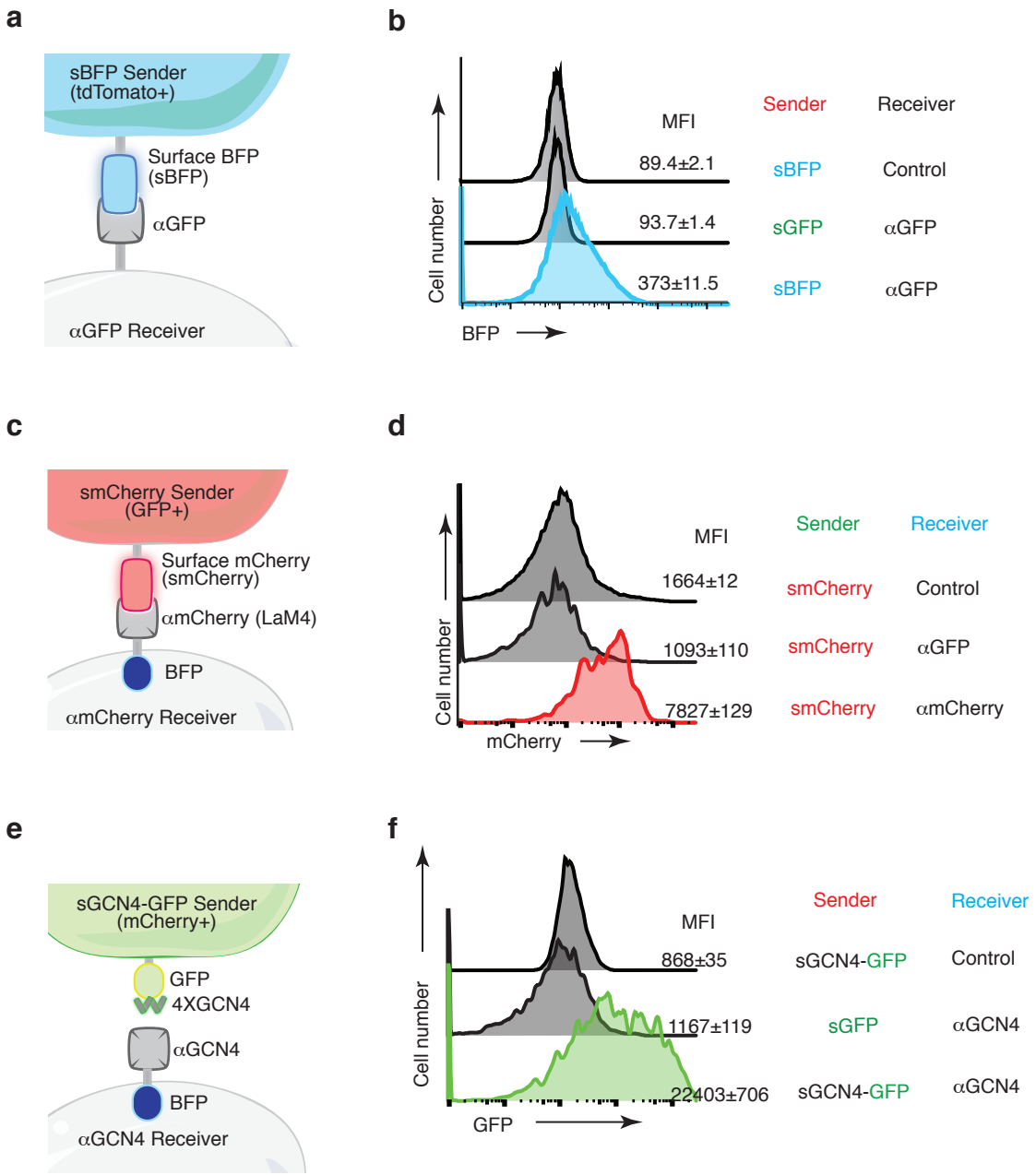

Supplementary Figure 4. X-baToN systems enable fluorescent labeling via various antigen-nanobody/scFV pairs.

a. Schematic of the surface BFP (sBFP)-baToN system. Sender cell (marked by intracellular tdTomato) expresses sBFP and receiver cell expresses α GFP.

b. The cross reactivity of αGFP with BFP allow BFP to be transferred from sBFP sender to αGFP receiver cells. sBFP senders and αGFP receivers were co-cultured at 1:1 ratio for 24 hours. Receivers were defined as toTomato^{neg}PI^{neg} cells. BFP MFI of receiver cells is shown as mean +/- SD of triplicate cultures.

c. Schematic of the surface mCherry (smCherry)-baToN system. Sender cell (marked by intracellular GFP) expresses smCherry and receiver cell expresses αmCherry (tagged by intracellular BFP)

d. The pairing between mCherry and αmCherry enable mCherry transfer from smCherry 293 Sender cells to αmCherry-expressing 293 Receiver cells. smCherry senders are not able to transfer mCherry to αGFP receiver cells. smCherry sender cells were co-cultured with αGFP or αmCherry receiver cells at a 1:1 ratio for 24 hours. Receivers were defined as GFP^{neg}BFP^{pos} cells. mCherry MFI of receiver cell is shown as mean +/- SD of triplicate cultures. smCherry 293 sender is not able to transfer mCherry to αGFP 293 receiver.

e. Schematic of the surface GCN4 (sGCN4)-baToN system. Sender cells (marked by intracellular 2A-mCherry) express cell surface 4X GCN4 peptide fused with GFP. Receiver cells express a cell surface anti-GCN4 single-chain variable fragment (scFV; αGCN4, tagged by intracellular BFP).

f. The pairing between GCN4 and αGCN4 enables co-transfer of GFP from 4X sGCN4-GFP senders to αGCN4 receivers 24 hours after co-culture at a 1:1 ratio. Receivers were defined as mCherry^{neg}PI^{neg}BFP^{pos} cells. GFP MFI of receiver cell is shown as mean +/- SD of triplicate cultures. sGFP sender are not able to transfer GFP to αGCN4 receivers.

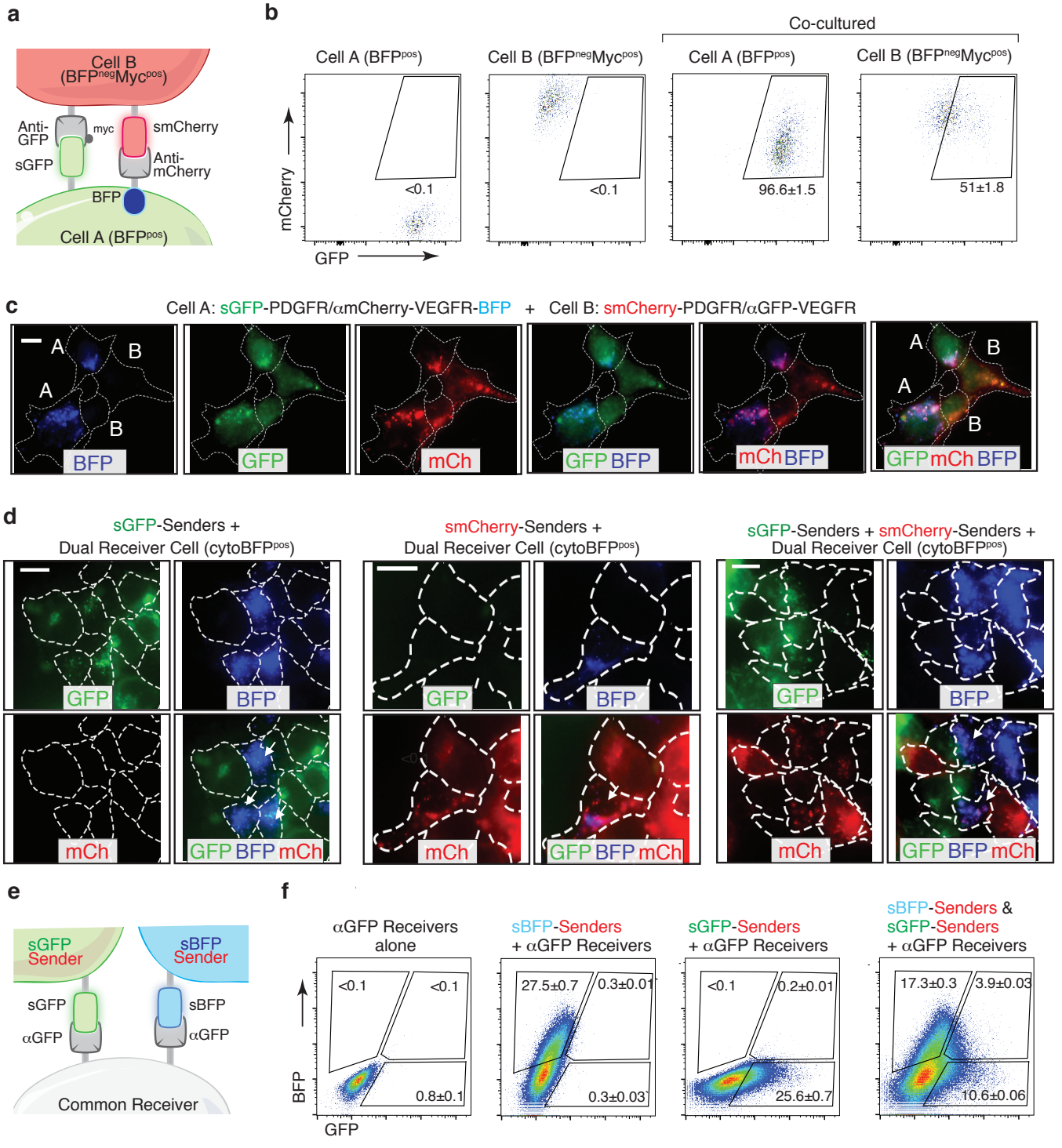

Supplementary Figure 5. Dual color-baToN systems enable labeling in complex cell-cell interaction systems.

a. Diagram of the Reciprocal-baToN system. Cell A expresses sGFP and αmCherry (tagged by intracellular BFP), Cell B expresses smCherry and α GFP (tagged by Myc-tag).

b. Representative FACS plots of cell A and cell B monocultures (left 2 panels) and after co-culture at a 5:1 ratio for 24 hours. Percent of labeled cells is indicated as mean +/- SD of triplicate cultures.

c. Representative image of reciprocal labeling of cell A and cell B co-cultured for 24 hours. Cells are outlined with a white dashed line. Cell A is BFP and GFP double positive and Cell B is mCherry positive. Touched cell A is BFP, GFP and mCherry triple positive and touched cell B is GFP and mCherry double positive (pointed out by white letter). Scale bar: 10 µm.

d. Representative image of dual receiver cells co-cultured with indicated sender cells. Cells are outlined with a white dashed line. Dual receiver cells are BFP positive and sender touched dual receiver cells are pointed out by white arrows. Scale bar: 10 µm.

e. Diagram of the BFP/GFP AND gate-baToN system. sBFP sender cells express intracellular Tomato and surface BFP, sGFP sender cells express intracellular Tomato and surface GFP. Common receiver cells expressed αGFP.

f. Representative FACS plots of common receiver 293 cells cultured with the indicated Tomato^{pos} sender cells at 1:1 (for single sender cell) or 1:1:1 (for dual sender cells) ratios. Receiver cells were gated as Tomato^{neg}PI^{neg}. Percent of labeled common receiver cells after 24 hours of co-culture is indicated as mean +/- SD of triplicate cultures.

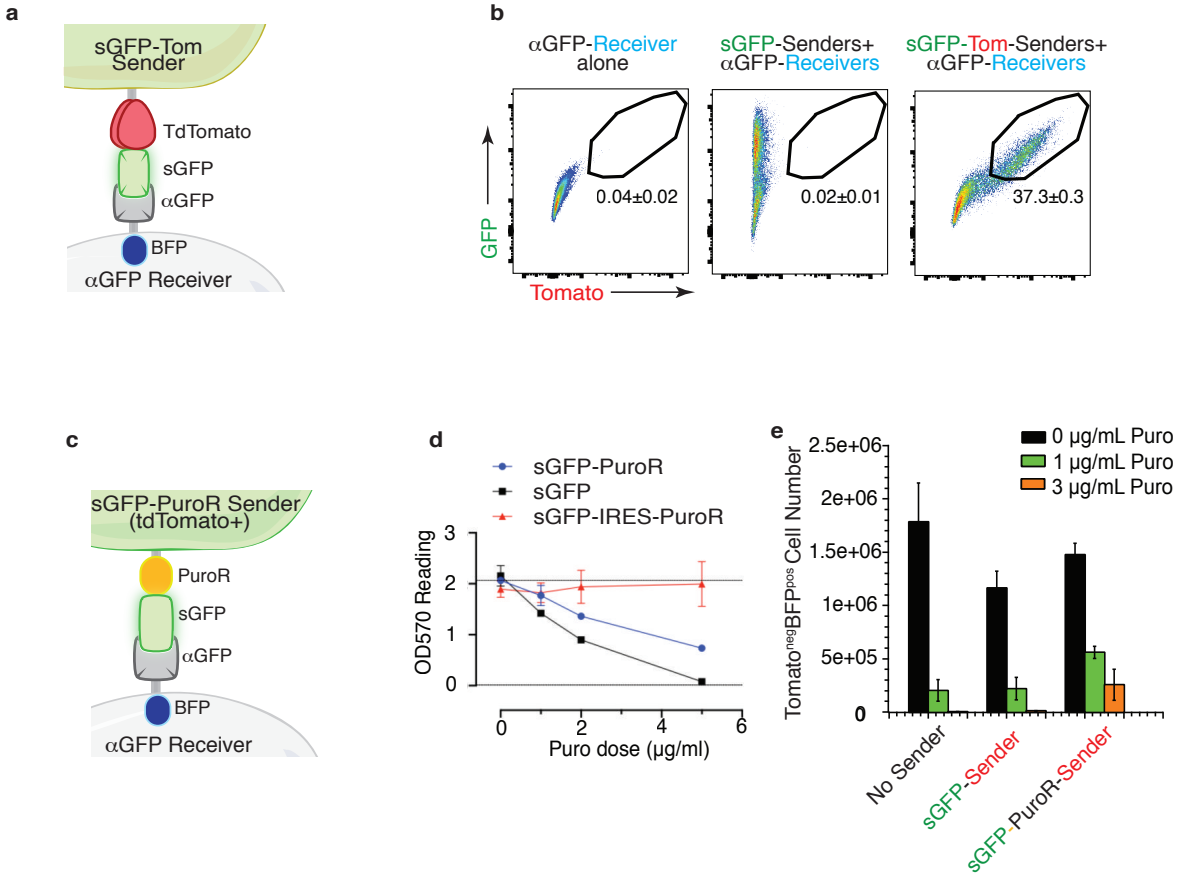

Supplementary Figure 6. Using the G-baToN system to co-transfer cargo protein into touched receiver cells.
a. Diagram of surface tdTomato-GFP (sGFP-Tom) co-transfer into touched receiver cells. Sender cell expresses sGFP-tdTomato and receiver cell expresses αGFP (tagged by intracellular BFP).
b. Representative FACS plots of αGFP 293 receiver cells cultured with the indicated sender cells at 1:1 ratio for 24 hours. Percent of GFP/Tomato dual labeled receiver cells is indicated as mean +/- SD of BFP^{pos} cells from triplicate cultures.
c. Diagram of GFP-PuroR co-transfer system. Sender cell expresses surface GFP associated with PuroR (marked by intracellular tdTomato), receiver cell expresses αGFP (tagged by intracellular BFP). PuroR: Gcn5-related N-acetyltransferase.
d. 293 Sender cells expressing sGFP-PuroR are only modestly resistant to puromycin treatment. 293 cells were transfected with plasmids as indicated. 24 hours after transfection, 293 cells were treated with different doses of puromycin for 24 hours. Cell number was assessed by measuring spectrophotometrically at 570 nm (OD570) after crystal violet staining.
e. Co-transfer of GFP-PuroR from sGFP-PuroR sender cells to αGFP 293 receiver cells confers puromycin resistance to receiver cells. Control, sGFP or sGFP-PuroR sender cells were co-cultured with αGFP 293 receiver cells for 24 hours at a 4:1 ratio before treatment with different dose of puromycin for 48 hours. $tdTomato^{neg}PI^{neg}BFP^{pos}$ cell numbers were counted via FACS.

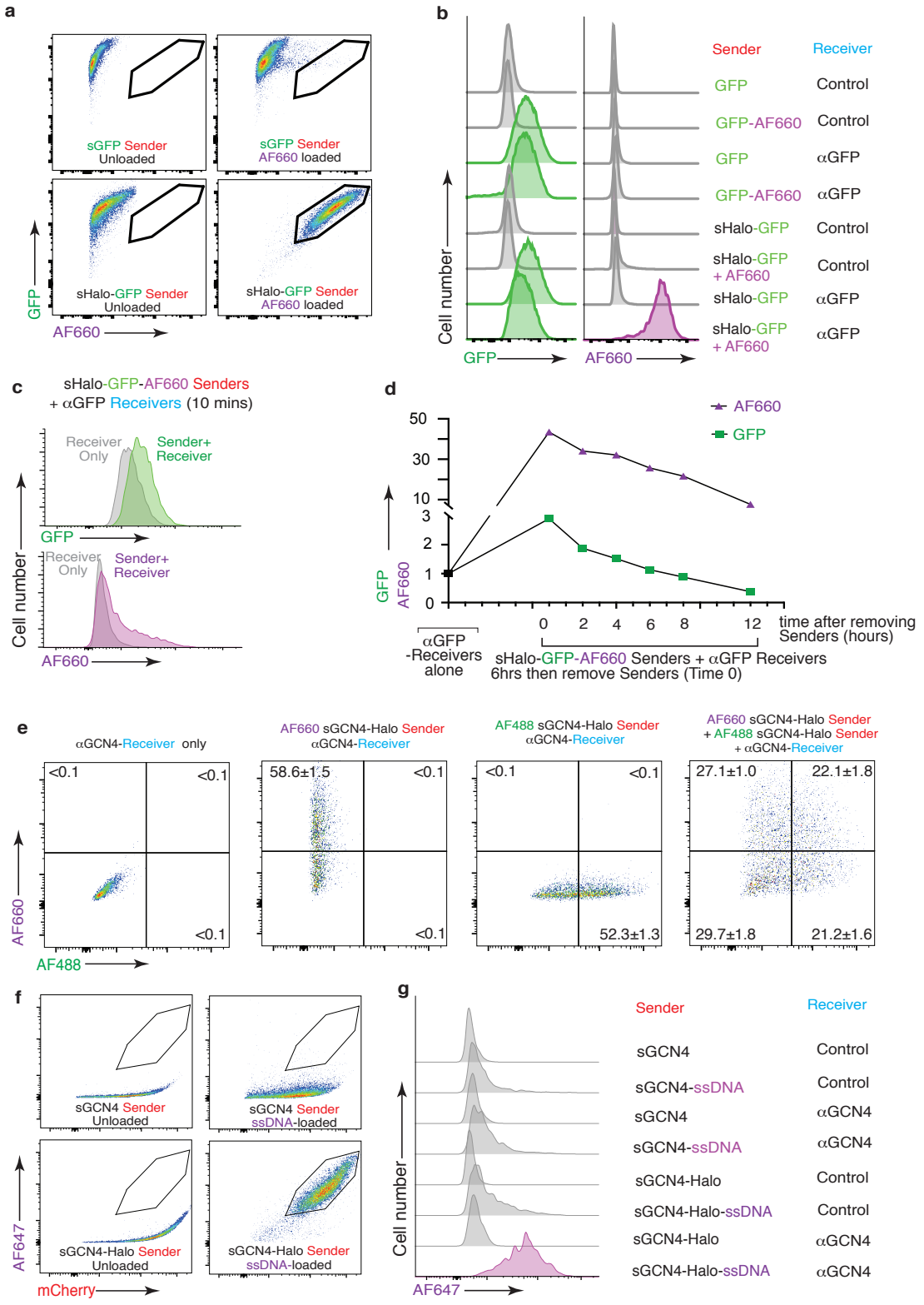

Supplementary Figure 7. The Halotag-baToN system enables touching based co-transfer.

a. Labeling HaloTag-expressing sender cells with AF660 fluorophore. Representative FACS plots of KP (lung adenocarcinoma) sender cells expressing either sGFP or sGFP-sHaloTag incubated with AF660-conjugated HaloTag ligand for 5 minutes on ice. AF660 specifically labeled sHaloTag-GFP sender cells but not sGFP sender cells.

b. Representative histogram of GFP and AF660 intensity in αGFP 293 receiver cells cultured with HaloTag-GFP sender cells at a 1:1 ratio for 6 hours (complete experiment results for Figure 2d). Receivers were defined as $mCherry^{neg}PI^{neg}BFP^{pos}$ cells.

c. AF660 transfer to αGFP 293 receiver cell is rapid after cell-cell interaction. AF660 MFI shift was detected after mixing sHalo-GFP senders and αGFP receivers and co-culture for 10 minutes. AF660 MFI shift was more dramatic than GFP. Receivers were defined as $mCherry^{neg}PI^{neg}BFP^{pos}$ cells.

d. Slower AF660 quenching in touched receiver cells after removing sHalo-GFP senders. After 6 hours co-culture, GFP/AF660 positive receiver cells were purified via FACS. Analysis of GFP/AF660 MFI in purified receiver cells showed rapid GFP degradation but slower AF660 quenching. Receivers were defined as $mCherry^{neg}PI^{neg}BFP^{pos}$ cells.

e. Representative FACS plots of αGCN4 receiver cells co-cultured with the indicated sender cells at 1:1 (for single sender cell) or 1:1:1 (for dual sender cells) ratios. Percent of labeled receiver cells (gated as $mCherry^{neg}PI^{neg}BFP^{pos}$) after 6 hours of co-culture is indicated as mean +/- SD of triplicate cultures.

f. Loading of sender cells with ssDNA. Representative FACS plots of 293 sender cells expressing either sGCN4 or sGCN4-Halo were loaded with 5' HaloTag-ligand, 3' biotin dual conjugated ssDNA (21nt), then stained with Avidin-AF647. AF647 specifically labeled loaded sGCN4-Halo sender cells but not sGCN4 sender cells.

g. Representative histogram of AF647 intensity in control or αGCN4 293 receiver cells cultured with sGCN4 or sGCN4-Halo sender cells at a 1:1 ratio for 6 hours (complete experiment results for Figure 2h). Receivers were defined as $mCherry^{neg}PI^{neg}BFP^{pos}$ cells.

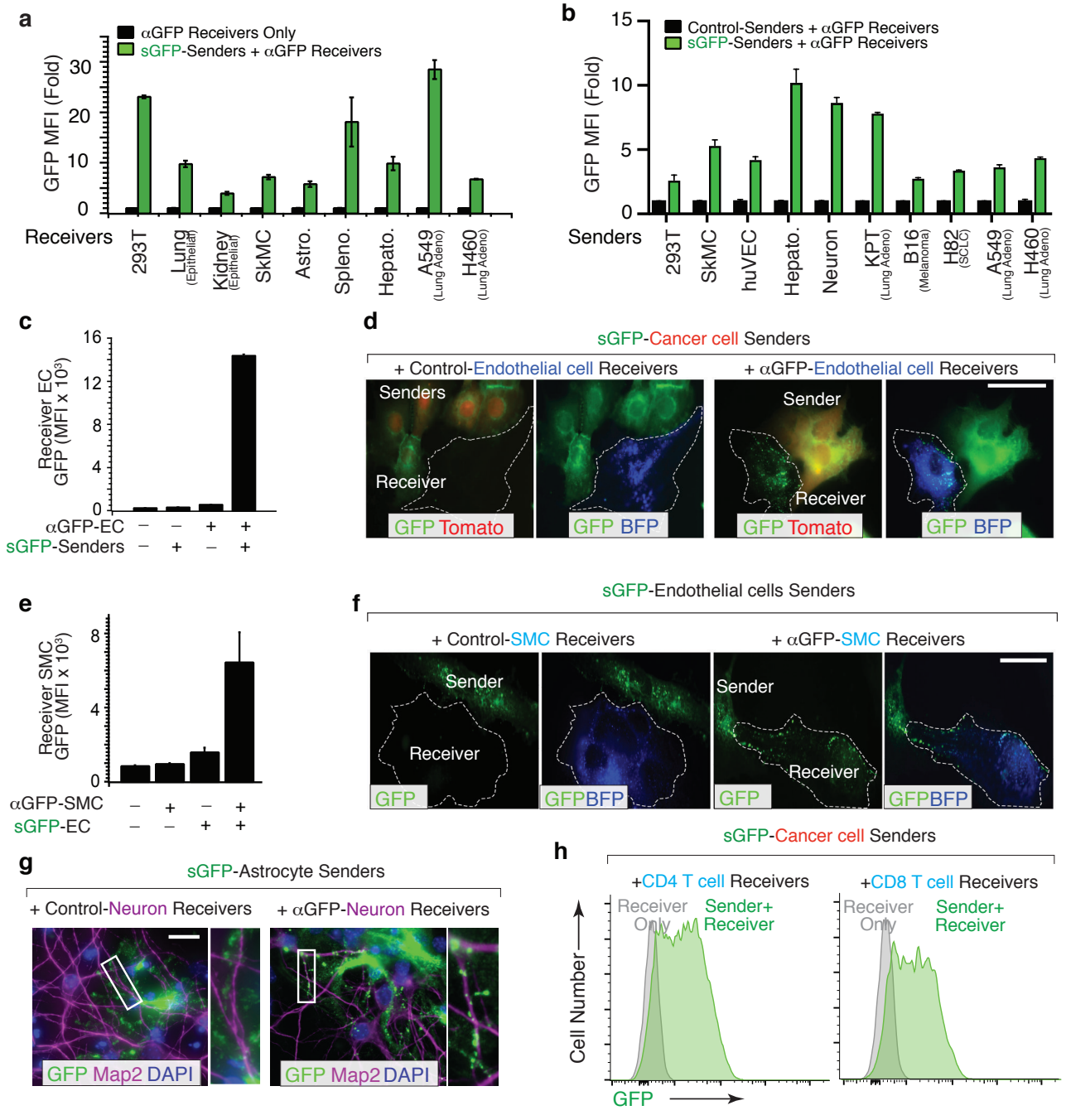

Figure 3. G-baToN is a generalized system that can be used for touching-based labeling between various cell types.
a. Many different cell lines and primary cell types can serve as receiver cells. Receiver cells expressing αGFP were co-cultured with sGFP-expressing KPT sender cells for 24 hours. MFI of GFP on Tomato^{neg}PI^{neg}BFP^{pos} receiver cells was assessed by FACS analysis and is shown as fold change relative to monocultured receiver cells. For lung epithelial cells and kidney epithelial cells MFI of GFP on Tomato^{neg}PI^{neg}BFP^{pos}EpCAM^{pos} cells is shown as mean +/- SD of triplicate cultures. SkMC: skeletal muscle cells. Astro: Astocytes. Hepato: hepatocytes. Spleno: splenocytes.
b. Many different cell lines and primary cell types can serve as sender cells. Sender cells expressing sGFP were co-cultured with αGFP 293 receiver cells for 24 hours. MFI of GFP on mCherry^{neg}PI^{neg}BFP^{pos} receiver cells was assessed by flow cytometry and is shown as fold change relative to monocultured 293 receiver cells. Mean +/- SD of triplicate cultures is shown.
c, d. G-baToN can detect cancer cell-endothelial cell (EC) interactions. HUVECs expressing αGFP were co-cultured with or without Tomato^{pos} sGFP-expressing lung cancer sender cells at a 1:1 ratio for 24 hours. MFI of GFP on PI^{neg}Tomato^{neg}BFP^{pos}CD31^{pos} Receiver cells was assessed by flow cytometry and is shown as mean +/- SD of triplicate cultures (**c**). Representative images of Tomato^{pos} sGFP-expressing lung cancer sender cells co-cultured with either control HUVEC receiver cells (HUVECs expressing BFP) or αGFP HUVEC receiver cells at a 1:1 ratio for 24 hours (**d**). Scale bars = 50 µm.
e,f. G-baToN can detect endothelial cell (EC)-smooth muscle cell (SMC) interactions. Primary human umbilical artery smooth muscle cells (HUASMC) expressing αGFP were co-cultured with or without sGFP-expressing HUVEC senders cells at a 1:1 ratio for 24 hours. MFI of GFP on PI^{neg}BFP^{pos} receiver cells was assessed by flow cytometry and is shown as mean +/- SD of triplicate cultures (**e**). Representative images of sGFP-expressing HUVEC sender cells co-cultured with either control HUASMC receiver cells (expressing BFP) or αGFP HUASMC receiver cells at a 1:1 ratio for 24 hours (**d**). Scale bars = 50 µm.
g. Representative images of sGFP-expressing astrocyte sender cells co-cultured with either control neuron receivers or αGFP neuron receivers at a 1:2 ratio for 24 hours. Neurons were stained with Microtubule Associated Protein 2 (Map2). Scale bars = 50 µm. Higher magnification of the boxed areas are shown on the right.
h. G-baToN can detect cancer cell-T cell interactions. Primary human CD4^{pos} (left) or CD8^{pos} (right) T cells were co-cultured with sGFP-expressing lung cancer sender cells (A549 cells) at a 2:1 ratio for 24 hours. Receivers were defined as mCherry^{neg}Near-IR^{neg}BFP^{pos}CD4^{pos}/CD8^{pos} T cells.

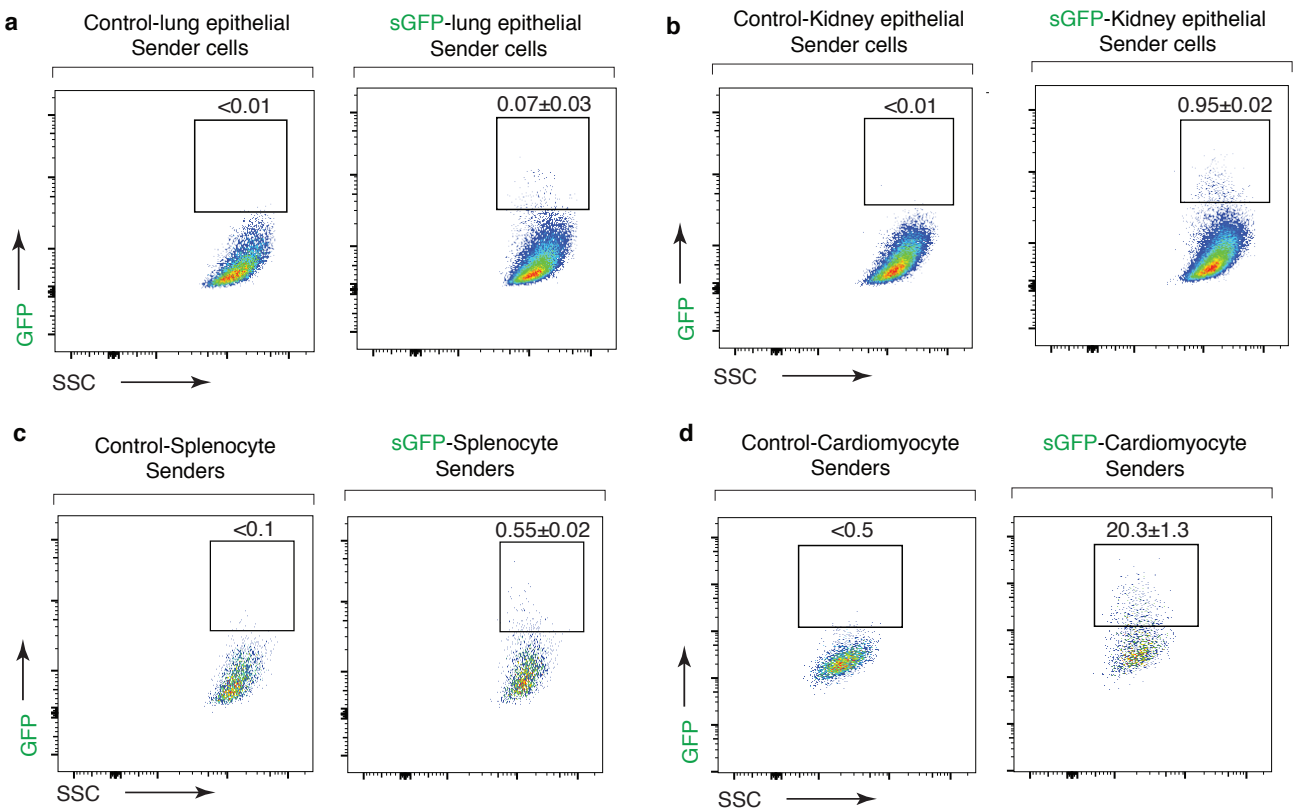

Supplementary Figure 8. Diverse primary mouse cells expressing sGFP can transfer GFP to αGFP 293 receivers.
Different primary sender cells were first sorted based on their cell surface markers, then transduced with lentiviral vectors expressing sGFP before being co-cultured with αGFP 293 receiver cells for 24 hours. Percentage of mCherry^{neg}PI^{neg}BFP^{pos}GFP^{pos} receiver cells was assessed by flow cytometry. For each primary sender, approximate sGFP^{pos} sender : αGFP^{pos} receiver ratio is indicated: **a**. Lung epithelial cells (1:180) (sorted EpCam^{pos} cells from dissociated adult lung); **b**. Kidney epithelial cells (1:20) (sorted EpCam^{pos} cells from dissociated adult kidney); **c**. Splenocyte (1:20); **d**. Cardiomyocyte (1:5) (sorted Sirpa^{pos} cells from dissociated adult heart). Percent of labeled cells is indicated as mean +/- SD of triplicate cultures.

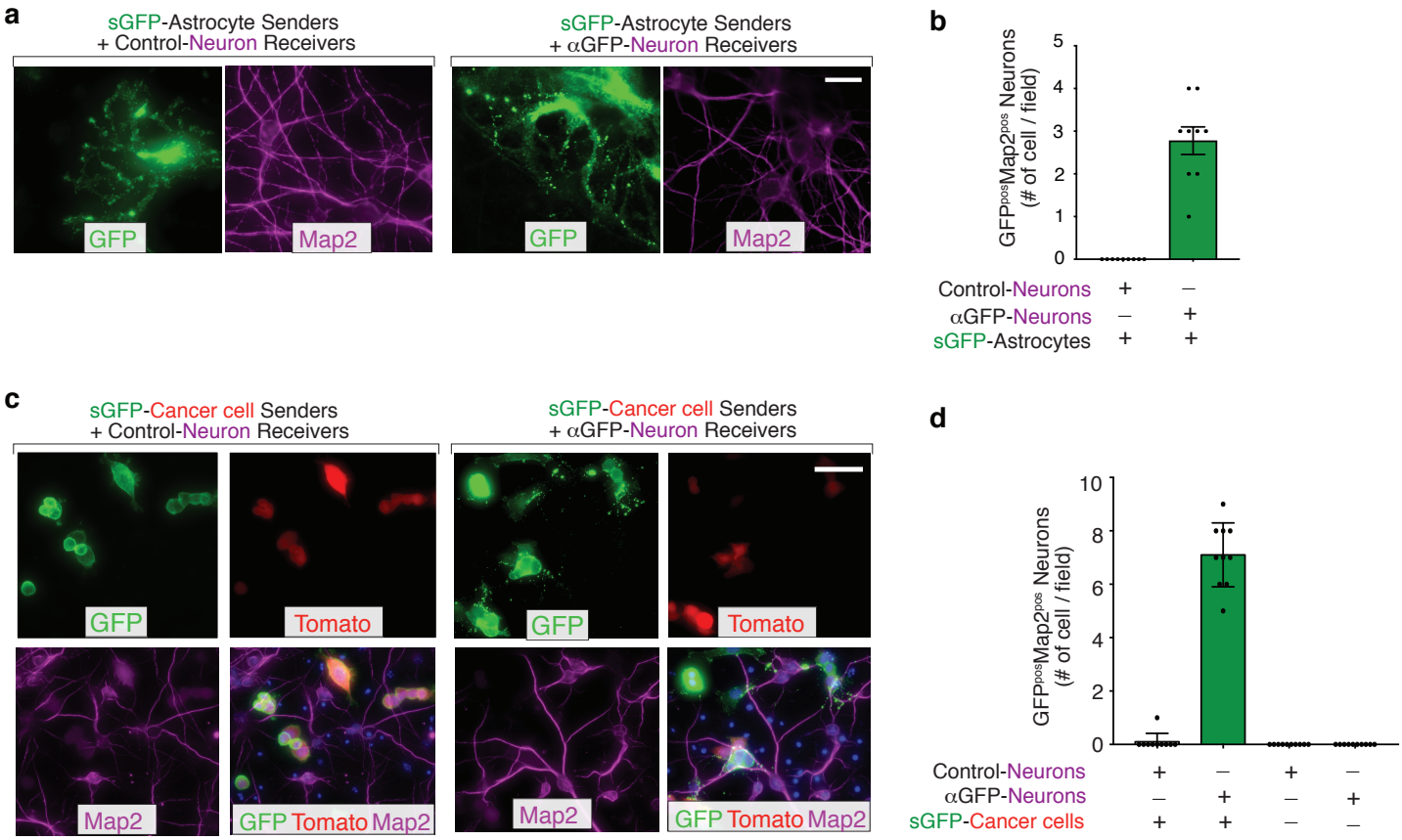

Supplementary Figure 9. G-baToN can detect neuron-astrocyte, neuron-cancer cell interactions.
a. Split channels for Figure 3g. Scale bars = 50 µm.
b. Quantification of Figure 3g using images from 10 different fields. Each dot represents a field. The bar indicates the mean +/- SD. GFP^{pos} neurons were defined as $Map2^{pos}$ cells with GFP.
c. Representative image of neuron and cancer cell interactions. Scale bars = 50 µm.
d. Quantification of supplementary Figure 9c using images from 10 different fields. Each dot represents a field. The bar indicates the mean +/- SD. GFP^{pos} neurons were defined as $Map2^{pos}tdTomato^{neg}$ cells with GFP.

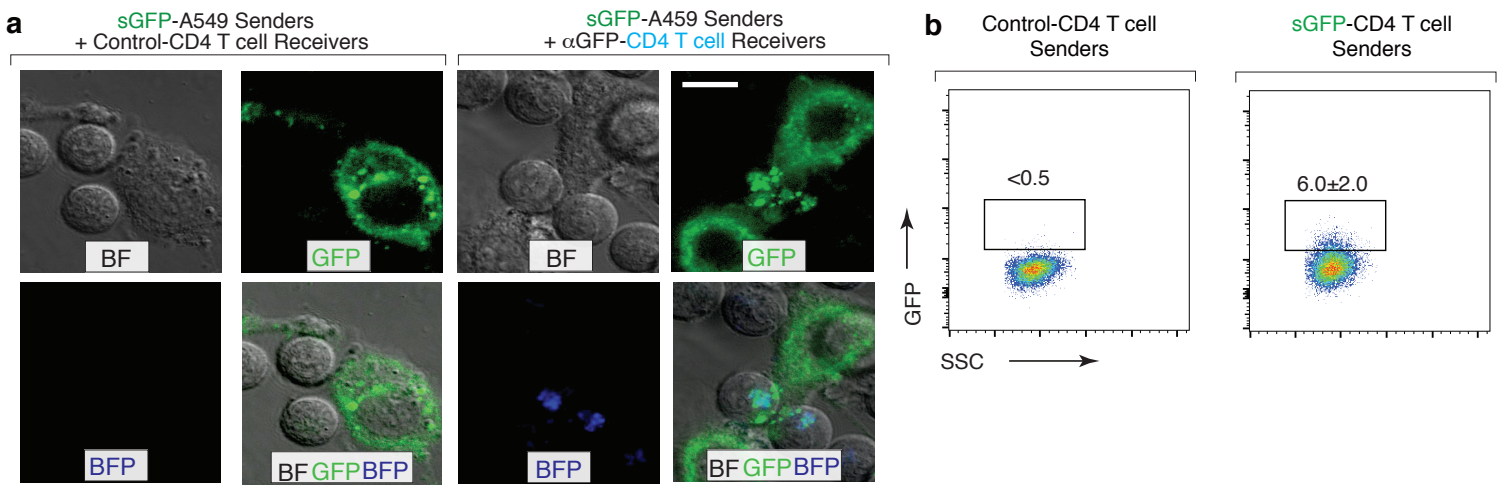

Supplementary Figure 10. G-baToN can detect CD4 T cell-A549 cancer cell interactions.
a. Representative image of A549 cell and CD4 T cell interactions. Scale bars = 10 µm.
b. Primary human $CD4^{pos}$ T cells expressing sGFP can transfer GFP to αGFP A549 cells after co-culture at a 1:1 ratio for 24 hours. Receivers were defined as $mCherry^{neg}NearIR^{neg}CD4^{neg}BFP^{pos}$ cells.